

Systematic Review Dental Implants

The role of artificial intelligence in implant dentistry: a systematic review

G. Vázquez-Sebrango^{a,b}, E. Anitua^b,
 I. Macía^{c,d}, I. Arganda-Carreras^{a,e,f,g}

^aDepartment of Computer Science and Artificial Intelligence, University of the Basque Country (UPV/EHU), Donostia-San Sebastián, Spain; ^bBTI Biotechnology Institute, Vitoria, Spain; ^cVicomtech Foundation, Digital Health and Biomedical Technologies Department, San Sebastián, Spain; ^dBiodonostia Health Research Institute, Bioengineering Area, eHealth Group, San Sebastián, Spain; ^eDonostia International Physics Centre (DIPC), San Sebastián, Spain; ^fIkerbasque, Basque Foundation for Science, Bilbao, Spain; ^gBiofisika Institute, Leioa, Spain

G. Vázquez-Sebrango, E. Anitua, I. Macía, I. Arganda-Carreras: *The role of artificial intelligence in implant dentistry: a systematic review. Int. J. Oral Maxillofac. Surg.* 2025; xx: 1–25. © 2025 The Authors. Published by Elsevier Inc. on behalf of International Association of Oral and Maxillofacial Surgeons. This is an open access article under the CC BY license (<http://creativecommons.org/licenses/by/4.0/>).

Abstract. The aim of this systematic review was to comprehensively analyse recent studies on the application of artificial intelligence (AI) in dental implantology. The PRISMA guidelines were followed. Five databases were accessed: Scopus, Web of Science, MEDLINE/PubMed, IEEE Xplore, and JSTOR. Documents published between 2018 and October 15, 2024 relating to AI and implantology were considered. Exclusions encompassed reviews, opinion articles, books, conference references, studies using AI as a supplementary method, AI for teaching implant dentistry, and AI for implant fabrication, prosthesis, or design. A total of 120 relevant papers were included. Risk of bias was assessed using PROBAST. Findings demonstrated extensive utilization of AI in various aspects of dental implantology: guided surgery, diagnosis, classification of oral structures, bone classification, classification of dental restorations, implant classification, implant planning, and implant prognosis. Deep learning algorithms were employed in 89.2% of studies, predominantly utilizing image data (72.0% two-dimensional images and 28.0% three-dimensional images). Publications doubled in 2022 compared to the previous year and have remained consistent since. Despite growth, the field remains relatively underdeveloped. However, with advancements in technology and data quality, substantial progress is anticipated in forthcoming years. Remarkably, 11 studies were found to have a high risk of bias.

Keywords: Artificial intelligence; Dental implants; Dental implantation; Neural networks (computer); Machine learning; Systematic review.

Accepted for publication 9 April 2025
 Available online xxxx

Artificial intelligence (AI) has emerged as a disruptive technology with the potential to revolutionize various fields, including dentistry. AI is an extensive field of computer science that focuses on creating algorithms that simulate human intelligence, performing cognitive tasks such as visual perception,

speech recognition, decision-making, and natural language processing¹.

AI is under extensive research in medicine, and several applications have been tested in dentistry, in the fields of oral cancer, periodontitis, dental caries, diseases of the dental pulp and periapical lesions, dental implants, and

orthodontics, among others². Notably, AI-enabled automatic segmentation has shown great promise in improving the accuracy and efficiency of procedures in craniofacial surgery³.

Machine learning (ML) is a category of AI that focuses on the development and implementation of computer

systems capable of learning from data without explicit programming instructions. It achieves this by employing sophisticated parametric algorithms and statistical models that adapt to the training data through algorithmic training. These models are designed to identify patterns within the data and provide estimates for unseen samples, facilitating predictive and decision-making capabilities.

Deep learning is a specialized sub-field of ML that uses artificial neural networks with multiple layers to effectively process and analyse vast amounts of unstructured data, including images, free text, signals, and voice. Its popularity and success stem from its remarkable ability to efficiently perform high-level cognitive tasks, such as image classification and object or pattern identification, even at the pixel level. One of its key strengths lies in conducting feature extraction and classification simultaneously, making it well-suited for analysing unstructured data⁴.

Deep learning excels at characterizing and encoding intricate patterns that may remain imperceptible to human observers. This capability enables it to reveal complex and subtle patterns hidden within the data⁵. Common algorithms used in deep learning include convolutional neural networks (CNNs) for image-related tasks, recurrent neural networks (RNNs) for sequential data, and generative adversarial networks (GANs) for generating new data instances.

Furthermore, the interaction between human operators and the neural network is an important aspect that influences the effectiveness and application of these systems. In the context of dental applications, considering human interaction becomes crucial, as it plays a vital role in fine-tuning and optimizing the performance of the neural network for specific tasks.

Dental implants have emerged as a widely accepted and effective solution for restoring oral function and enhancing aesthetics in patients with missing teeth. A successful outcome of implant procedures relies on critical factors, including bone quality, soft tissue thickness, and occlusion, among others. With the rapid advancements in AI, there is great potential for leveraging this technology to aid dentists in

evaluating these crucial factors, thereby facilitating a more personalized and precise approach to implant planning, placement, and diagnosis.

Several systematic reviews have explored AI in implant dentistry and have provided a broad overview of deep learning in periodontology and implantology^{6,7}. More recent reviews have evaluated CNNs, focusing on their performance in specific applications, such as identifying dental implants⁸⁻¹⁰ or planification¹¹.

The current review expands on these foundations by offering a more extensive classification of AI applications and a broader evaluation of algorithms, encompassing both traditional ML and advanced deep learning techniques. A detailed risk of bias assessment was conducted, and the review provides a comparative analysis of methodologies, offering a comprehensive perspective that complements and extends the findings of previous studies.

The primary objective of this study was to conduct a comprehensive analysis of the progress and advancements made in the field of AI in implantology. The aim was to investigate the specific topics and areas that have been explored through existing research, while considering factors such as publication dates, types and quantities of data used, specific AI technologies employed, the evaluation of potential biases, and study outcomes. The ultimate goal of this work was to assess whether further research is needed in these domains. Therefore, the null hypothesis posited that there is no need for further research in the field of AI in implantology.

A PICOT question was formulated to delineate the scope of this systematic review: (P, patient/population/problem) What is the available evidence on the use of AI in implant dentistry, (I, intervention) in terms of various implementations and approaches of AI used for implant interventions, (C, comparison) comparing the outcomes with the conventional approaches without AI utilization, (O, outcome) in relation to the success rate of dental implants, accuracy in treatment planning and accuracy in the drilling protocol, accuracy in implant positioning, accuracy of the surgical guide, accuracy in the classification of oral structures, accuracy in diagnosis, accuracy in bone

classification, accuracy in implant classification, and efficiency in implant placement, (T, time) in studies published during the period from 2018 to October 15, 2024?

Materials and methods

Five databases were accessed: Scopus, Web of Science, MEDLINE/PubMed, IEEE Xplore, and JSTOR. The search strategy included documents published between 2018 and October 15, 2024 related to AI and implantology in all languages. The following words were selected as keywords related to AI: 'AI', 'artificial intelligence', 'machine learning', and 'deep learning'. The following keywords related to implantology were selected: 'dental implant', 'dental implants', 'dental implantology'. Hence, a search was conducted for studies containing one of the terms selected as relating to AI and one of the terms selected as relating to implantology. The search criteria used in each of the databases are listed in Table 1.

The following inclusion criteria were applied for the studies analysed in this review: (1) the investigation must pertain to the application of AI in various domains of implantology, encompassing clinical practice aspects such as surgical procedures and their planning, the identification of pertinent oral structures for surgery, diagnosis related to implant requirements, implant prognosis, treatment, and analysis, or identification of the implant itself; (2) studies published within the time period 2018 to October 15, 2024.

The exclusion criteria were defined as follows: (1) reviews: studies falling under the category of review articles; (2) opinion articles: articles presenting opinions or editorials; (3) books: any literature classified as books; (4) conference references: references derived from conference proceedings or abstracts without full-length articles; (5) supplementary use of AI: studies that used AI as a supplementary tool rather than the primary focus of the investigation; (6) AI for teaching implant dentistry: studies centred on the use of AI for teaching implant dentistry; (7) AI for implant fabrication, prosthesis, or design: studies that focused on the use of AI for the design, prosthesis, or

manufacturing process of dental implants; (8) studies written in languages other than English, Spanish, German, French, Italian, or Portuguese.

After conducting the initial search, duplicate studies were removed to ensure data integrity. Subsequently, the abstracts of the remaining studies were thoroughly examined, and the inclusion and exclusion criteria were meticulously applied.

The selection process was conducted by two independent reviewers, and any discrepancies in study selection were resolved through mutual discussion. In the event of an unresolved disagreement, the study in question was jointly reviewed by both reviewers, and if consensus was still not reached, a third reviewer made the final decision. The exclusion criteria were applied in the following sequence: books, opinion articles, conference papers without study information, studies not related to dental implantology (including AI for teaching implantology and design and fabrication), studies not related to AI or related to the supplementary use of it, reviews, and other exclusion criteria. A kappa index of 0.96 was obtained for this stage of the selection process.

Additionally, a relevant study suggested by the website from which the selected articles were downloaded was identified and included for comprehensive analysis.

The full texts of all remaining documents were then evaluated, and those

studies that did not meet the criteria were discarded. In this way, the total number of studies eligible for analysis was obtained. The kappa index in this phase was 0.87.

Following the study selection, a single reviewer was responsible for the extraction and analysis of information from the selected studies.

Subsequently, comprehensive data extraction was conducted for each of the selected studies, with a specific focus on the following key variables: year of publication, primary topic of investigation, AI technology and model type used, study objectives, types of data utilized (including two-dimensional (2D) or three-dimensional (3D) images, or structured data (text and numerical variables)), and input data, as well as the corresponding performance metrics and risk of bias assessment.

The studies were classified into eight primary topics based on their content: guided surgery, diagnosis, classification of oral structures, bone classification, classification of dental restorations, implant classification, implant planning, and implant prognosis. After data extraction, the collected information was thoroughly analysed to derive relevant conclusions.

The risk of bias assessment for the included studies was conducted using the PROBAST tool¹².

The level of evidence of each included study was evaluated according

to the Oxford Centre for Evidence-Based Medicine (OCEBM) Levels of Evidence (<https://www.cebm.ox.ac.uk/resources/levels-of-evidence/ocebml-levels-of-evidence>).

This systematic review adhered to the guidelines outlined in the PRISMA protocol (Preferred Reporting Items for Systematic Reviews and Meta-Analyses)¹³. The methodology of the review was registered in the international prospective register of systematic reviews, PROSPERO (CRD42024607237).

Results

The search was performed using the criteria outlined in Table 1, resulting in 1356 studies. Among them, 579 duplicates were removed, and one study was excluded due to being written entirely in Chinese. After reviewing the abstracts of the remaining 776 studies, the exclusion criteria were applied.

The search and the first selection of articles according to their abstracts was conducted by two independent reviewers, and they agreed regarding the inclusion of all but four of the studies. Upon jointly analysing the remaining studies, a mutual decision was made to include them in the review. Consequently, the kappa index for the first study inclusion according to the abstracts was 0.96. In cases where articles could be excluded for multiple reasons, reaching a consensus between

Table 1. Search strategy.

Database	Database search algorithm	Additional date filter	Additional filters
Scopus	Line 1: (artificial AND intelligence) OR ai OR (machine AND learning) OR (deep AND learning) AND Line 2: dental AND (implant OR implants OR implantology)	2018–October 15, 2024	TITLE-ABS-KEY
Web of Science	((artificial AND intelligence) OR ai OR (machine AND learning) OR (deep AND learning)) AND (dental AND (implant OR implants OR implantology))	2018–October 15, 2024	Topic (title + Abstract + Indexing) All databases; All collections
MEDLINE/ PubMed	((artificial AND intelligence) OR ai OR (machine AND learning) OR (deep AND learning)) AND (dental AND (implant OR implants OR implantology))	2018–October 15, 2024	All fields
IEEE Xplore	((("All Metadata":dental) AND ("All Metadata":implant*)) AND (("All Metadata":artificial intelligence) OR ("All Metadata":ai) OR ("All Metadata":machine learning) OR ("All Metadata":deep learning)))	2018–October 15, 2024	All metadata
JSTOR	((artificial AND intelligence) OR ai OR (machine AND learning) OR (deep AND learning)) AND (dental AND (implant OR implants OR implantology))	2018–October 15, 2024	Subject: technology, public health, health sciences, general science, biological sciences Only journals

the two reviewers was essential in determining the specific reason for exclusion. This collaborative approach ensured that the exclusion criteria were consistently applied and minimized potential discrepancies in the study selection process.

Following this stage, 137 studies were eligible for full-text assessment, with all except five obtained and reviewed. After a thorough examination of the full texts, two studies were excluded for not being related to implantology and 11 studies were excluded as AI was not the primary focus of the investigation; rather, it was only considered as a secondary aspect in these studies.

In addition, one relevant article that could not be retrieved from the initially selected databases using the established criteria was added¹⁴. This article was suggested by the website from which the selected articles were downloaded, as it exhibited similarities to the included studies. The full-text review was also conducted by two independent reviewers, and the kappa index was 0.87.

Finally, a total of 120 studies were included in this systematic review¹⁴⁻¹³³. Fig. 1 provides a flow chart of the

step-by-step process for the selection of these studies.

Detailed characteristics of the 120 selected studies, along with the extracted data, are presented, by topic, in Tables 2A–H.

Topic

The studies could be classified into the following eight categories according to their topic: guided surgery; diagnosis; classification of oral structures; bone classification; classification of dental restorations; implant classification; implant planning; implant prognosis.

Five studies were on guided surgery (Table 2A)¹⁵⁻¹⁹. These studies focused on the optimization of the drilling protocol¹⁵ in 3D radiographic images, and in structured data for improving the dimensional accuracy of the surgical guide¹⁶ and predicting the optimal implant position¹⁷. Two studies also predicted the implant position from 3D images by converting them to series of 2D images^{18,19}.

Thirteen studies were on diagnosis (Table 2B)²⁰⁻³². These studies focused on the image-based classification of different oral structures and

rehabilitations for diagnosis including dental implants²⁰⁻³¹, the detection of fractured dental implants³², and diagnosis of periodontal bone loss, peri-implantitis, and periodontitis^{21,26,29}. Three of the studies used commercial software^{22,25,30}. All of these studies used radiographic images with deep learning classification algorithms, and all except one, which used 3D radiographs, used 2D images.

Twenty studies were on the classification of oral structures (Table 2C)³³⁻⁵². All of these studies dealt with image-based semantic segmentation (pixel-level labelling) of the maxillary sinus³³⁻³⁶ and mandibular canal^{33,37-52}. All of the studies used radiograph images.

Bone classification was the subject of eight studies^{14,53-59} (Table 2D). Most of these studies tried to classify the bone type in radiographic images⁵³⁻⁵⁷. However, one study tried to detect osteoporosis in 3D radiographic images⁵⁸, while another evaluated the efficacy of alveolar ridge preservation in reducing the need for bone augmentation by using structured data¹⁴ and one measured the thickness of the anterior maxilla in 3D radiographs⁵⁹.

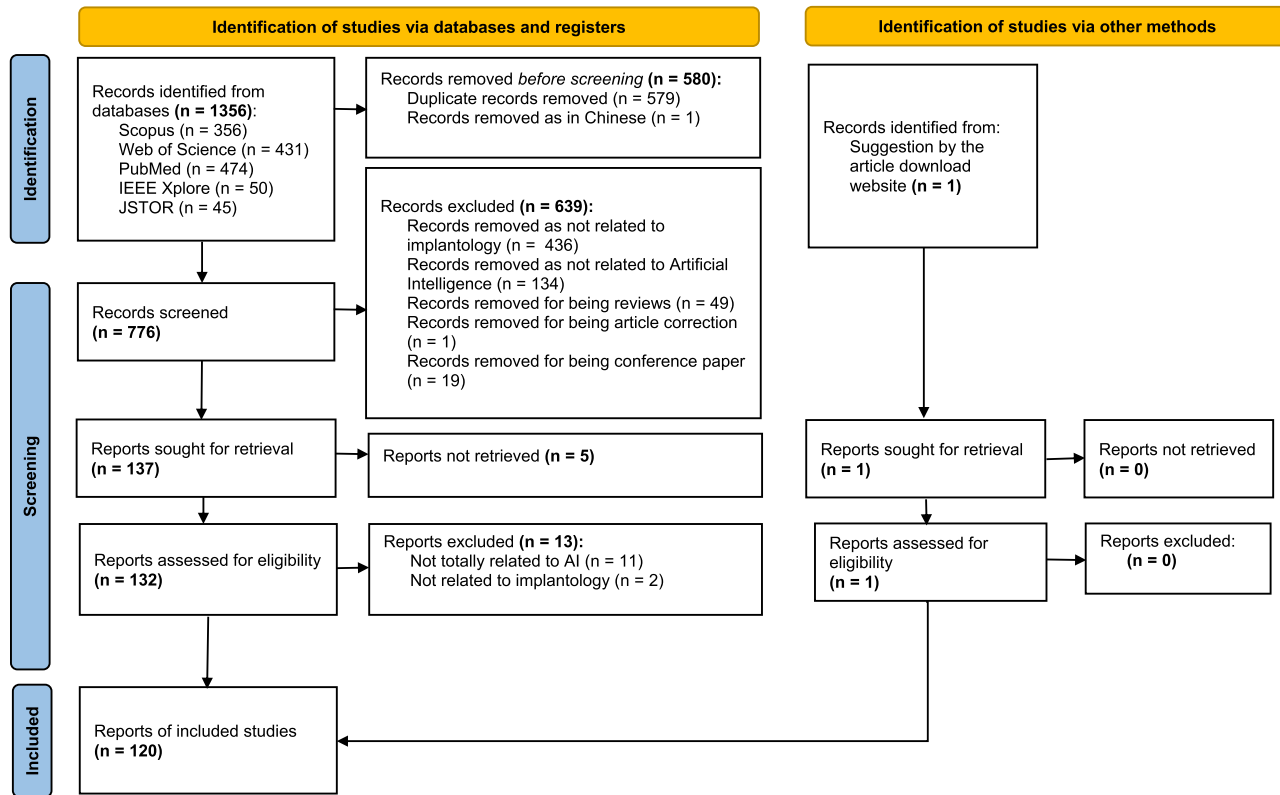


Fig. 1. PRISMA 2020 flow diagram of the search and selection process for this review.

Table 2A. Key characteristics of the studies in the 'guided surgery' group.

Year Ref.	Technology AI model	Purpose	Data	Results	OEL
2022 ¹⁵	DL LeNet-5-based model	Identify drilling protocol	1200 CBCT	Accuracy: 93.8%; sensitivity: A (97.5%), B (95%), C (85%); precision: A (86.7%), B (92.7%), C (100%); F1 values: A (91.8%), B (93.8%), C (91.9%); AUC-ROC values: A (98.6%), B (98.6%), C (99.4%)	3b
2022 ¹⁶	DL ANN Model 5	Dental guide accuracy	1944 SD	Accuracy ANN Model 5: 99%	3b
2020 ¹⁷	DL W-J48, NB, SVM, KNN, NNSRM, GRNN, GLCTNN	Predict implant location	1276 SD	Precision: W-J48 (96.57%), NB (96.98%), SVM (97.45%), KNN (97.89%), NNSRM (98.46%), GRNN (98.89%), GLCTNN (99.43%) Recall: W-J48 (96.23%), NB (96.47%), SVM (97.21%), KNN (97.53%), NNSRM (98.13%), GRNN (98.43%), GLCTNN (99.03%)	3b
2023 ¹⁸	DL TCSIoT – ResNet50	Identify 3D implant position	154 CBCT	AP75: 20.4%; F1: 20.1%	3b
2024 ¹⁹	DL ImplantFormer – ViT-Base-ResNet50	Predict implant position	154 CBCT	AP75: 13.7%; F1: 13.6%	3b

3D, three-dimensional; ANN, artificial neural network; AP75, average precision at an intersection over union (IoU) threshold of 0.75; AUC-ROC, area under the receiver operating characteristic curve; CBCT, cone beam computed tomography; DL, deep learning; F1, F1 score; GLCTNN, guided local search with continuous time neural network; GRNN, generalized regression neural network; KNN, k-nearest neighbours; NB, naïve Bayes; NNSRM, nearest neighbour with structural risk minimization; OEL, Oxford Centre for Evidence-Based Medicine level of evidence; SD, structured data; SVM, support vector machine.

Classification of the dental restoration was the subject of nine studies (Table 2E)^{60–68}. All of the studies used classification algorithms to identify dental restorations, including dental implants, in 2D radiographs.

Implant classification was reported in 29 studies (Table 2F)^{69–97}. All of these studies used 2D radiograph images and aimed to identify the brand and type of implant by using classification algorithms^{69–96}. One study uses 3D radiographs but converted them to 2D for the analysis⁹⁷.

Fifteen studies were on implant planning (Table 2G)^{98–112}. Most of the studies used radiographic image data to identify dental structures for optimal implant planning^{98–110}. Others evaluated the use of AI for cone beam computed tomography (CBCT) and intraoral scan overlap¹¹¹ and implant depth planning¹¹².

The implant prognosis was investigated in 21 studies (Table 2H)^{113–133}. These studies focused on predicting long-term outcomes of dental implants by identifying their failure or success^{113–120}, the identification of a ridge deficiency around dental implants¹²¹, bone loss in 2D radiographs^{122–125}, peri-implant soft tissue status in 3D radiographs¹²⁶, peri-implantitis from structured data^{127,128}, peri-implantitis from 2D radiographs¹²⁹, implant need based on structured data¹³⁰, implant stability in

3D radiographs¹³¹, postoperative discomfort using structured data¹³², and the prediction of osteonecrosis based on structured data¹³³.

Publication date

A significant increase in the number of publications was observed over the study period (2018–2024). The number of studies published in 2022 was double that published in each of the previous 2 years and 10 times the number published in 2018 and 2019 together. In 2023, only four more articles were published when compared to 2022, and 2024 showed a slightly lower count than in the previous 2 years, although the search included data only up to October. The number of articles appears to have remained relatively stable since 2022. This information is presented in Fig. 2.

Type of data

Training data for an AI model refers to the input examples used to teach the model patterns and relationships. In the context of image data, 2D images involve pixel intensity information, while 3D images incorporate depth or volumetric data. Structured data, on the other hand, consists of organized, tabular information with clear relationships between variables.

Of the 120 studies, 107 predominantly used image data (89.2%), while the other 13 studies employed structured data (text and numerical variables) (10.8%). Further examination of the image data revealed that 72.0% (77/107) of the studies used 2D images; the remaining 28.0% (30/107) focused on 3D images. Additional information on the types of data used can be found in Fig. 3.

Data range

There was a lack of uniformity in the number of data samples used for training, primarily influenced by the availability of quality data and, for image datasets, the time required for labelling. For 2D images, the average number of images used was 10,077, with a broad range spanning from 44 to 157,495 images. Regarding 3D images, the average number was 1162, with the range being 20 to 19,350 images. In the case of structured data, the average number of patients or samples considered was 1330, with a range of data points spanning from 24 to 8513 images.

AI technology

In this systematic review, ML emerged as the predominant AI technology employed by all of the included studies,

6 Vázquez-Sebrango et al.

Table 2B. Key characteristics of the studies in the 'diagnosis' group.

Year Ref.	Technology AI model	Purpose	Data	Results	OEL
2021 ²⁰	DL Faster R-CNN; GoogLeNet Inception-v2	Classification of 10 oral structures	1084 PR	Sensitivity: crown (0.9674), implant (0.9615), impacted tooth (0.9658), pontic (0.7738), caries (0.3026), calculus (0.0934) Precision: pontic (0.8783), implant (0.9259), implant-supported crown (0.8947), root (0.6764), caries (0.5096), calculus (0.1923) F1: implant (0.9433), crown (0.9122), implant-supported crown (0.8947), calculus (0.1257), caries (0.3798), residual root (0.7419)	3b
2022 ²¹	DL Faster R-CNN	Classification of implants and peri-implant tissues	300 PA	Classification: precision 0.977, recall = 0.992, F1 = 0.984 Localization: mean IoU = 0.907	3b
2022 ²²	DL Apox (Promaton) software	Accuracy of AI diagnostic tool	120 PR	Classification and localization: AP50, 0.996; AP75, 0.967 Kappa: 1.0 (data collectors) Identification: TP (19.06%), TN (77.34%), FP (1.15%), FN (2.46%) Overall sensitivity, 0.89; overall specificity, 0.98; PPV, 0.94; NPV, 0.97; LR+, 44; LR-, 0.001; diagnostic effectiveness, 0.96 Sensitivity; specificity: presence of teeth (0.95; 0.90), implants (0.84; 0.99), residual roots (0.68; 0.98), root canal treatments (0.83; 0.99), crowns (0.93; 0.99), fillings (0.61; 0.99)	3b
2022 ²³	DL Hybrid, AlexNet, GoogLeNet, VGG19, ResNet50, ResNet101	Classification of treatment	1400 PR	Segmentation accuracy: 98.75% Accuracy after enhancement: hybrid method (75.53%), AlexNet (97.13%), GoogLeNet (98.2%), VGG19 (96.88%), ResNet50 (97.45%), ResNet101 (97.38%)	3b
2022 ²⁴	DL NASNet; AlexNet	Classification of treatment	116 PR	Accuracy: NASNet + data augmentation (96.51%); NASNet without data augmentation (93.36%); AlexNet + data augmentation (93%)	3b
2022 ²⁵	DL Denti.Ai software	Evaluation of web-based AI for dental structures and treatments	300 PR	Metal restorations: sensitivity (85.48%), specificity (87.50%), PPV (82.8%), NPV (42.51%), AUC-ROC (0.869) Resin-based restorations: sensitivity (41.11%), specificity (93.30%), PPV (90.24%), NPV (87.50%), AUC-ROC (0.672) Endodontic treatment: sensitivity (91.9%), specificity (100%), PPV (100%), NPV (94.62%), AUC-ROC (0.960) Crowns: sensitivity (89.53%), specificity (95.79%), PPV (89.53%), NPV (95.79%), AUC-ROC (0.927) Implants: sensitivity (100%), specificity (100%), PPV (100%), NPV (100%), AUC-ROC (1)	3b
2023 ²⁶	DL YOLOv3, IU, Canny edge detection	Detection of peri-implant bone resorption, implant, and crown	2920 PA and BW	Crown and implant: mAP50 (0.537–0.898) IU: line lifting ($P = 0.0106$; statistical average/standard deviation in pixels = 2.75/1.01); significant point detection ($P = 0.0213$; statistical average/standard deviation in pixels = 2.63/1.28)	3b
2023 ²⁷	DL U-Net	Segmentation and classification of oral structures	7696 PR	Dice: teeth (0.95), crown-bridge restorations (0.93), dental implants (0.94), restorative fillings (0.87), dental caries (0.88), residual roots (0.78), root canal fillings (0.78)	3b
2023 ²⁸	DL U-Net	Dental implant and crown segmentation	280 CBCT	Implant: accuracy (0.99); precision (0.98); recall (0.99); DSC (0.98); IoU (0.97) Implant + crown: accuracy (0.99); Precision (0.95); recall (0.99); DSC (0.97); IoU (0.95)	3b
2023 ²⁹	DL YOLOv2, AlexNet	Classification of periodontal damage around implants	406 PA	Implant position: accuracy (0.893); damage detection accuracy (0.904)	3b
2023 ³⁰	DL Diagnocat	Dental AI-software diagnosis evaluation	100 PR	Kappa > 0.81; kappa dental implants: 0.898	3b
2024 ³¹	DL YOLOv4 + ResNet18, GhostNet	Classification of dental treatment and diagnosis	661 PR	Dental implant: AP 8.72%; tooth: AP 78.05%; root canal treatment: AP 82.63%	3b
2021 ³²	DL VGGNet-19, GoogLeNet Inception-v3, DCNN	Detection of broken implants	445 PR and PA	DCNN: AUC-ROC 0.972, SE 0.014, sensitivity 0.866, specificity 0.966, YI 0.833 GoogLeNet Inception-v3: AUC-ROC 0.967, SE 0.015, sensitivity 1.000, specificity 0.866, YI 0.866 VGGNet-19: AUC-ROC 0.929, SE 0.037, sensitivity 0.933, specificity 0.933, YI 0.866	3b

AP, average precision; AP50, average precision at an IoU threshold of 0.50; AP75, average precision at an IoU threshold of 0.75; AUC-ROC, area under the receiver operating characteristic curve; BW, bitewing radiograph; DCNN, deep convolutional neural network; DL, deep learning; DSC, Dice similarity coefficient; F1, F1 score; FN, false negative; FP, false positive; IoU, intersection over union; LR+, positive likelihood ratio; LR-, negative likelihood ratio; mAP50, mean average precision at an IoU threshold of 0.50; NPV, negative predictive value; OEL, Oxford Centre for Evidence-Based Medicine level of evidence; PA, peri-apical radiograph; PPV, positive predictive value; PR, panoramic radiograph; R-CNN, region-based convolutional neural network; SE, standard error; TN, true negative; TP, true positive; YI, Youden index.

Table 2C. Key characteristics of the studies in the 'classification of oral structures' group.

Year Ref.	Technology AI model	Purpose	Data	Results	OEL
2021 ³³	DL Panoptic-DeepLab	Detect different oral structures	51 PR	AP: normal tooth (0.520), treated tooth (0.316), dental implant (0.414)	3b
2022 ³⁴	DL U-Net	Maxillary sinus segmentation	19,350 CBCT	AI model: DSC (0.9090 ± 0.1921), HD (2.7013 ± 4.6154) With post-processing: DSC (2.7013 ± 4.6154), HD (2.1470 ± 2.2790)	3b
2023 ³⁵	DL YOLOv5; ResNet50	Detect maxillary sinus abnormalities	2000 CBCT	AUC-ROC (0.953), AUC-PRC (0.882), precision (0.833), recall (0.87), specificity (0.948), accuracy (0.93), F1 (0.851)	3b
2024 ³⁶	DL Swin-UNETR, 3D U-Net	Accurate segmentation of alveolar bone, teeth, and maxillary sinus	451 CBCT	Dice: 96.5% (teeth), 95.4% (alveolar bone), 93.6% (maxillary sinus), 94.8% (mandibular canal) HD: 1.62 mm for teeth	3b
2020 ³⁷	DL ResNet50, VGG16, VGG19	Detection of sectional plane where mandibular canal path is maximally observed	500 2D CT	$\Delta t = 9.73 \pm 6.40$ mm; $\delta\theta = 1.32 \pm 0.869$ mm; CRR = 0.886 ± 0.149 mm	3b
2020 ³⁸	DL Similar to U-Net	Mandibular canal segmentation	637 CBCT	DSC: 0.57 ± 0.08 left, 0.58 ± 0.09 right MCD: 0.61 ± 0.16 mm left, 0.50 ± 0.19 mm right ASSD: 0.45 ± 0.12 left, 0.45 ± 0.11 mm right RHD: 1.40 ± 0.63 mm left, 1.38 ± 0.47 mm right	3b
2021 ³⁹	ML AdaBoost M2 Ensemble	Detect IAC without the foramen	1440 PR	AdaBoost M2 Ensemble: precision (100%), recall (92.3%), F1 (96%), accuracy (96%) Ensemble: precision (91.66%), recall (100%), F1 (95.6%), accuracy (96%)	3b
2022 ⁴⁰	DL U-Net	Segmentation of mandibular canal compared to radiologists	1132 CBCT	$P < 0.001$	3b
2022 ⁴¹	DL Dental-Yolo (YOLOv4)	Alveolar bone and mandibular canal detection	1064 2D CBCT	Alveolar bone precision: 99.37%; mandibular canal precision: 99.55%; total precision: 99.46%; mIoU: 81.33%; BFLOPS: 6.83	3b
2022 ⁴²	DL U-Net	Mandibular canal segmentation	1347 CBCT	mIoU: 0.795; precision: 0.69; recall: 0.83; Dice: 0.751; F1: 0.759	3b
2022 ⁴³	DL HOG; LBP; GLCM; MELMANN	IAC detection	220 PR	Overall accuracy; cross entropy: HOG (71%; 1.98); LBP (74%; 1.789); GLCM (50%; 2.689); HOG+LBP+GLCM (c) (84%; 0.6943); HOG+LBP+GLCM (all) (89%; 1.5467); HOG+LBP+GLCM (c, c, e, h) (92%; 0.18079); maxHOG+maxLBP+GLCM (c) (92%; 0.68959); maxHOG+maxLBP+GLCM (all) (89%; 0.5305); maxHOG+maxLBP+GLCM (c, c, e, h) (96%; 0.16533)	3b
2022 ⁴⁴	DL U-Net	Mandibular canal segmentation	20 CBCT	HD95% mm (0.5371); Dice (0.8591); IoU (0.754); recall (0.8877); precision (0.8355)	3b
2023 ⁴⁵	DL U-Net	Mandibular incisive canal segmentation	200 CBCT	Mean DSC (0.876); mean IoU (0.781); mean RMSE (0.267); mean precision (0.852); mean recall (0.902); mean accuracy (0.998); consistency (1)	3b
2023 ⁴⁶	DL U-Net	Alveolar bone and mandibular canal segmentation	563 2D CBCT	Simultaneous segmentation: IoU (0.85) Separate segmentation: alveolar bone IoU (0.98), mandibular canal IoU (0.81)	3b
2023 ⁴⁷	DL U-Net	Segmentation of the mandibular canal and its anterior loop	313 CBCT	Mandibular canal with anterior loop: IoU (0.659); DSC (0.792); precision (0.677); recall (0.961); accuracy (0.998); HD95% mm (0.428) Mandibular canal: IoU (0.654); DSC (0.789); precision (0.668); recall (0.970); accuracy (0.997); HD95% mm (0.429)	3b
2023 ⁴⁸	DL EfficientUNet	IAC segmentation with ambiguity classification	1366 PR	Automatic segmentation: DSC 85.7% (95% CI 75.4–90.3%), precision 84.1% (95% CI 78.4–89.3%), recall 87.7% (95% CI 77.7–93.4%) Group 1: DSC (82.7%), precision (80%), recall (86.2%) Group 2: DSC (85.3%), precision (84.1%), recall (87.3%) Group 3: DSC (87.2%), precision (86%), recall (88.8%) Group 4: DSC (89.1%), precision (88%), recall (90.1%)	3b
2024 ⁴⁹	DL Software: coDiagnostiX; BlueSkyPlan	Accuracy of commercial software in segmentation of the mandibular canal	104 CBCT	RMSE: mean (3.5 mm), lowest in the middle section of the mandibular canal	3b

Table 2C. (Continued)

Year Ref.	Technology AI model	Purpose	Data	Results	OEL
2024 ⁵⁰	DL YOLOv7-tiny, RPIFormer, CycleGAN	Segmentation of mandibular third molar and canal	450 PR	2 sets: RPIFormer 92.93%; Dice 94.78% (third molar, mandibular canal), 87.21%, 90.18%	3b
2024 ⁵¹	DL U-Net, U-Net++, ResUNet, LinkNet, FPN	Segmentation of mental foramen	702 PR	U-Net (square mask): Dice 79.96%, IoU 76.69% U-Net (round mask): Dice 79.02%, IoU 67.76%	3b
2024 ⁵²	DL 2D U-Net, 3D U-Net	Segmentation of the mandibular canal	625 CBCT	Internal set: Dice 0.952, IoU 0.912, ASSD 0.046 mm, HD95% 0.325 mm External set: Dice 0.960, IoU 0.924, ASSD 0.040 mm, HD95% 0.288 mm	3b

Δt, Euclidean distance (mm); θ, rotation angle (°); 2D, two-dimensional; 3D, three-dimensional; 95% CI, 95% confidence interval; AP, average precision; ASSD, average symmetric surface distance; AUC-ROC, area under the receiver operating characteristic curve; AUC-PRC, area under the precision-recall curve; BFLOPS, billion of floating point operations per second; CBCT, cone beam computed tomography; CRR, canal region ratio; CT, computed tomography; DL, deep learning; DSC, Dice similarity coefficient; F1, F1 score; FPN, feature pyramid network; HD, Hausdorff distance; HD95%, 95th percentile Hausdorff distance; IAC, inferior alveolar nerve canal; IoU, intersection over union; MCD, mean curve distance; mIoU, mean intersection over union; ML, machine learning; OEL, Oxford Centre for Evidence-Based Medicine level of evidence; PR, panoramic radiograph; RHD, robust Hausdorff distance; RMSE, root mean square error.

indicating its central role in various classifications.

Of the analysed studies, a significant majority (89.2%) claimed to employ deep learning for their AI algorithms, highlighting the widespread recognition and use of this powerful approach in the field of implantology.

Regarding the specific AI algorithms, the most frequently used algorithms and the number of studies in which they were used are outlined below, for those that were used in more than two studies.

ResNet (n = 30)

ResNet is a deep CNN architecture proposed by He et al.¹³⁴ in 2016. It uses skip connections to allow the network to learn residual mappings, which helps to avoid the vanishing gradient problem and enables the training of very deep networks with up to 152 layers¹³⁴. All of the studies that employed ResNet used images as input (80% of them in 2D and 20% in 3D), with an average number of images of 13,649.9.

R-CNN (n = 9)

R-CNN stands for region-based convolutional neural network, which is a CNN-based object detection method proposed by Girshick et al.¹³⁵ in 2014. It involves a two-stage process where regions of interest are first identified using a selective search algorithm, and then these regions are classified using a CNN¹³⁵. All of the studies that employed R-CNN used image data as

input (88.9% of them in 2D and 11.1% in 3D), with an average number of images of 2121.2.

GoogLeNet (n = 12)

GoogLeNet is a deep CNN architecture proposed in 2014 by Google. It uses a novel inception module that allows for efficient use of computing resources and has a significantly smaller number of parameters compared to previous models¹³⁶. All of the studies that used GoogLeNet employed image data as input (91.7% of them in 2D and 8.3% in 3D), with an average number of images of 5028.2.

VGG (n = 14)

VGG is a deep CNN architecture proposed by Simonyan and Zisserman in 2014¹³⁷. It consists of a series of convolutional and pooling layers with a fixed filter size of 3×3 , and is characterized by its depth, with up to 19 layers in its most complex version¹³⁷. All of the studies using VGG employed image data as input, with an average number of images of 3788.7.

YOLO (n = 19)

YOLO ('You Only Look Once') is a real-time object detection algorithm. Object detection is framed as a regression problem to spatially separated bounding boxes and associated class probabilities. A single neural network predicts bounding boxes and class probabilities directly from full images

in one evaluation. It was described by Redmon et al.¹³⁸ in 2015. All of the studies that used YOLO employed image data as input (94.7% of them in 2D and 5.3% in 3D), with an average number of images of 2662.1.

U-Net (n = 21)

U-Net was developed in 2015 for biomedical images. It is a fully CNN designed to achieve end-to-end semantic image segmentation, even when dealing with limited training samples. Its distinctive architecture features a U-shaped encoder-decoder design, incorporating four encoder blocks and four decoder blocks interconnected through a bottleneck or bridge¹³⁹. All of the studies that used U-Net employed image data as input (28.6% of them in 2D and 71.4% in 3D), with an average number of images of 1175.8.

AdaBoost (n = 3)

AdaBoost is a boosting algorithm proposed by Freund and Schapire in 1995¹⁴⁰. It is an ensemble learning method in which weak classifiers are combined to create a strong classifier. AdaBoost works by adjusting the weights of misclassified samples at each iteration to focus on hard examples, resulting in an effective algorithm for binary classification tasks¹⁴⁰. Two of the three studies (66.7%) using AdaBoost used structured data as input, while one (33.3%) used 2D images. The average number of data samples was 764.7.

Table 2D. Key characteristics of the studies in the 'bone classification' group.

Year Ref.	Technology AI model	Purpose	Data	Results	OEL
2022 ¹⁴	ML Logistic regression	Alveolar ridge preservation (ARP) vs unassisted socket healing (USH) to reduce the need for bone augmentation for implants	140 SD	Bone augmentation necessary in 60% (USH) and 11.4% (ARP) of the sites Most of these sites (64.2% USH and 87.5% ARP) had thin facial bone phenotype (< 1 mm) at baseline Need for ancillary bone augmentation: 17.8 times higher in sites with ARP therapy Additional bone augmentation reduced 7.7 times for every 1-mm increase in facial bone thickness (UHS and ARP) Best: 3D deep CNN, with accuracy of 99.1%	2b
2019 ⁵³	DL 3D CNN; SegNet; 2D CNN; NN; Haar-like feature	Classification of alveolar bone type	207 CBCT		3a
2021 ⁵⁴	DL YOLOv3-tiny; YOLOv2-tiny; YOLOv3	Automatic alveolar bone detection	800 CBCT	YOLOv2-tiny: TP (159), FP (5), FN (8); precision (0.97), recall (0.95), F1 (0.96), mAP (96.73%) YOLOv3: TP (164), FP (0), FN (3); precision (1), recall (0.98), F1 (0.99), mAP (98.6%) YOLOv3-tiny: TP (162), FP (4), FN (5); precision (0.98), recall (0.97), F1 (0.97), mAP (98.6%)	3b
2022 ⁵⁵	DL Nested U-Net	Implant site bone type classification	605 CBCT	HU means labelled by physicians: type I (1519), type II (920), type III (693), type IV (351), type V (195) HU means labelled by model prediction: type I (1520), type II (964), type III (648), type IV (352), type V (136)	3b
2023 ⁵⁶	DL QCBCT-NET (U-Net)	Validate the accuracy and reliability of bone density measurements and bone density classification	7500 2D CT + 2D CBCT	QCBCT images: RMSE (83.41 mg/cm ³), MAE (67.94 mg/cm ³), MAPE (8.32%) CAL_CBCT images: RMSE (491.15 mg/cm ³), MAE (460.52 mg/cm ³), MAPE (54.29%)	3b
2024 ⁵⁷	DL ResNet50	Classify bone quality from PR compared to CBCT values and surgeon's tactile assessment	2270 PR	AUC-ROC 0.762 Spearman correlation: CBCT $r = 0.702$; surgeon's tactile sense $r = 0.658$	3b
2020 ⁵⁸	DL BPANN	Osteoporosis detection	120 CBCT	Accuracy 97.917%, precision 0.96, recall 1, F1 0.97959	3b
2023 ⁵⁹	DL BCNN + VGG16, ResNet18, ResNet34, ResNet50, ResNet101, ResNeXt50	Thickness assessment of buccal bone using low-resolution CBCT	4000 CBCT	Best is BCNN-VGG16: accuracy 0.870, precision: 0.843, sensitivity: 0.701, specificity: 0.943, F1: 0.765, AUC-ROC 0.924, AUC-PRC:0.859; better than human metrics (visual estimation)	3b

2D, two-dimensional; 3D, three-dimensional; AUC-ROC, area under the receiver operating characteristic curve; AUC-PRC, area under the precision-recall curve; BCNN, binary complex neural network; BPANN, back propagation artificial neural network; CBCT, cone beam computed tomography; CNN, convolutional neural network; CT, computed tomography; DL, deep learning; F1, F1 score; FN, false negative; FP, false positive; HU, Hounsfield units; MAE, mean absolute error; mAP, mean average precision; MAPE, mean absolute percentage error; ML, machine learning; NN, neural network; OEL, Oxford Centre for Evidence-Based Medicine level of evidence; PR, panoramic radiograph; RMSE, root mean square error; SD, structured data; TP, true positive.

Support vector machine (SVM) ($n = 7$)

SVM is a supervised ML algorithm for classification and regression tasks, proposed by Cortes and Vapnik¹⁴¹ in 1995. SVM finds a hyperplane that separates the data into different classes with a maximum margin, which maximizes the generalization performance of the classifier¹⁴¹. Overall, 71.4% of the studies using SVM used structured data as input, while 28.6% of them used 2D images. The average number of data samples was 602.5.

Logistic regression ($n = 7$)

Logistic regression is a statistical linear model for binary classification tasks, proposed by Cox in 1958. Logistic regression models the probability of a binary event as a function of one or more independent variables and can manage both categorical and continuous data¹⁴². Of the studies using logistic regression, 57.1% used structured data as input, while 42.9% used 2D images. The average number of data samples was 516.6.

Random forest ($n = 5$)

Random forest is an ensemble learning algorithm proposed by Breiman in 2001¹⁴³. Random forest constructs multiple decision trees on random subsets of the training data and features and combines the predictions of these trees to obtain the final output¹⁴³. Eighty percent of the studies using random forest used structured data as input, while 20% of them used 2D images as input. The average number of data samples was 396.

Table 2E. Key characteristics of the studies in the 'classification of dental restorations' group.

Year Ref.	Technology AI model	Purpose	Data	Results	OEL
2020 ⁶⁰	DL ResNet; DenseNet; GoogLeNet	Dental restoration classification	3013 PR	Accuracy: GoogLeNet (89%), DenseNet (94%), ResNet (93%)	3b
2022 ⁶¹	DL Faster R-CNN ResNet50; Faster R-CNN ResNet101; Faster R-CNN Xception-101; Libra RCNN Xception-101; Faster R-CNN RegNetX 3.2GF; Cascade RCNN ResNet101; Dynamic R-CNN; SSD512 VGG16; YOLO DarkNet53; RetinaNet ResNet101	Dental restoration classification	123 PR	Faster R-CNN ResNet50 (mAP50: 0.958; mAP50-95: 0.677; average recall: 0.732) Faster R-CNN ResNet101 (mAP50: 0.930; mAP50-95: 0.705; average recall: 0.745) Faster R-CNN Xception-101 (mAP50: 0.941; mAP50-95: 0.682; average recall: 0.720) Libra RCNN Xception-101 (mAP50: 0.938; mAP50-95: 0.711; average recall: 0.767) Faster R-CNN RegNetX 3.2GF (mAP50: 0.973; mAP50-95: 0.723; average recall: 0.771) Cascade RCNN ResNet101 (mAP50: 0.917; mAP50-95: 0.689; average recall: 0.749) Dynamic R-CNN (mAP50: 0.934; mAP50-95: 0.688; average recall: 0.736) SSD512 VGG16 (mAP50: 0.875; mAP50-95: 0.623; average recall: 0.721) YOLO DarkNet53 (mAP50: 0.755; mAP50-95: 0.442; average recall: 0.605) RetinaNet ResNet101 (mAP50: 0.903; mAP50-95: 0.665; average recall: 0.751)	3b
2024 ⁶²	DL U-Net	Segment dental implants	300 PA	Accuracy 93.8%, precision 90%, recall 83%, F1 86%, IoU 86.4%, loss 21%	3b
2024 ⁶³	DL YOLOv8	Dental structures detection	1267 PR	mAP50: 0.806	3b
2024 ⁶⁴	DL DMAF-Net (based on YOLOv5s)	Detection of dental structures	1474 PR	mAP50: 91.8%, mAP50-95: 63.7%, F1: 90.08%, precision: 92.7%, recall: 87.6%	3b
2024 ⁶⁵	DL YOLOv5s, YOLOv7m, YOLOv8m	Detection and segmentation of dental structures	600 PR	YOLOv7m best in detection (recall 0.793, precision 0.779, mAP50 0.740, mAP50-95 0.481) YOLOv8m best in segmentation (recall 0.589, precision 0.755, mAP50 0.591, mAP50-95 0.272) YOLOv5s (recall 0.634, precision 0.781, mAP50 0.631, mAP50-95 0.392)	3b
2023 ⁶⁶	DL SFFNet	Segmentation of dental structures	1500 PR	Dice 95.46%, precision 96.53%, recall 95.76%, F1 96.11%	3b
2023 ⁶⁷	DL VGG-Net	Classification of dental structures	1000 PR	Classification accuracy for dentition 93.5%, prosthetic treatment 90.5%, tooth number 89.5%, implant status 89.5%, impacted wisdom tooth 69%, sex 75.5%, age 56%	3b
2023 ⁶⁸	DL YOLOv3, YOLOv4, YOLOv5, SSD, Faster-RCNN; AlexNet, BotNet, GoogLeNet, Inception-ResNet-v1, Inception-v3, MoileNet-v2, ResNet50, ShuffleNet-v2, VGG11, VGG13, VGG16, Vit-5, Xception	Detect and classify different oral structures	15,240 2D CT	Object detection Single implants: YOLOv5 precision 87.39%, F1 88.05%; Faster-RCNN recall 93.43% Double implants: Faster-RCNN precision 87.48%, F1 91.24% Compound implants: Faster-RCNN recall 94.64%, AP 97.84% Steel balls: Faster-RCNN recall 97.83%; YOLOv5 AP 97.24% Crowns and braces: Faster-RCNN recall 91.42%; YOLOv5 F1 78.45% Multi-object detection: Faster-RCNN mAP 91.63% Classification Single implants: GoogLeNet precision 99.14%, F1 95.82% Double implants: Inception-ResNet-v1 precision 85.26%; GoogLeNet recall 95.90% Compound implants: GoogLeNet F1 85.96%, recall 95.36%	3b

2D, two-dimensional; AP, average precision; CT, computed tomography; DL, deep learning; F1, F1 score; IoU, intersection over union; mAP, mean average precision; mAP50, mean average precision at an IoU threshold of 0.50; mAP50-95, average of the mean average precision calculated at varying IoU thresholds ranging from 0.50 to 0.95; OEL, Oxford Centre for Evidence-Based Medicine level of evidence; PA, peri-apical radiograph; PR, panoramic radiograph; R-CNN, region-based convolutional neural network.

Table 2F. Key characteristics of the studies in the 'implant classification' group.

Year Ref.	Technology AI model	Purpose	Data	Results	OEL
2020 ⁶⁹	DL DCNN Neuro-T	DI system classification compared to professionals	11,980 PR + PA	AUC-ROC, YI, sensitivity, and specificity: 0.954, 0.808, 0.955, 0.853. Best results: AI	3b
2020 ⁷⁰	DL CNN; VGG16; VGG19; finely tuned VGG16 and VGG19	Classification of 11 DI systems	8859 PR	CNN: recall (0.802), precision (0.842), accuracy (0.860), F1 (0.819) VGG16-transfer: recall (0.864), precision (0.888), accuracy (0.899), F1 (0.874) VGG16-fine tuning: recall (0.907), precision (0.928), accuracy (0.935), F1 (0.916) VGG19-transfer: recall (0.840), precision (0.873), accuracy (0.880), F1 (0.853) VGG19-fine tuning: recall (0.894), precision (0.913), accuracy (0.927), F1 (0.902)	3b
2020 ⁷¹	DL GoogLeNet Inception-v3	DI system classification	1206 PR	Diagnostic (%; 95% CI) Accuracy: 93.8% (87.2–99.4%), sensitivity: 93.5% (84.2–99.3%), specificity: 94.2% (83.5–99.4%), PPV: 92% (83.9–97.2%), NPV: 91.5% (80.2–97.1%) AUC-ROC: 0.918 (0.826–0.973) on NNA; 0.922 (0.831–0.964) on NBS; 0.909 (0.844–0.982) on SBL; 0.890 (0.783–0.945) on STL; 0.931 (0.867–0.979) on ZTSV; 0.911 (0.811–0.957) on ZSP	3b
2020 ⁷²	DL GoogLeNet Inception-v3	DI system classification compared to professionals	10,770 PA + PR	Model: AUC-ROC 0.971 (95% CI 0.963–0.978) Periodontist: AUC-ROC 0.925 (95% CI 0.913–0.935)	3b
2020 ⁷³	DL YOLOv3	DI system classification	1282 PR	TP: 0.50–0.82; AP: 0.51–0.85; mAP: 0.71, mIoU: 0.72	3b
2020 ⁷⁴	DL SqueezeNet; GoogLeNet; ResNet; MobileNet-v2	DI system classification	801 PA	Test accuracy; precision; recall; F1: SqueezeNet: 0.96; 0.96; 0.96; 0.96 GoogLeNet: 0.93; 0.92; 0.94; 0.93 ResNet18: 0.98; 0.98; 0.98; 0.98 MobileNet-v2: 0.97; 0.96; 0.96; 0.96 ResNet50: 0.98; 0.98; 0.98; 0.98	3b
2021 ⁷⁵	DL CNN	DI system classification	1800 PA	(%; 95% CI): Accuracy: 85.3 (78.4–90.5), sensitivity: 89.9 (81.1–95.6), specificity 82.4 (73.7–87.3), PPV 82.6 (74.1–86.6), NPV 88.5 (79.8–93.9)	3b
2021 ⁷⁶	DL DCNN Neuro-T	DI system classification compared to professionals	11,980 PA + PR	AI: mean accuracy 80.56% Professionals without AI: mean accuracy 63.13%, 77.67%, 67.94%, 57.81% Professionals with AI: mean accuracy 78.88%, 88.56%, 77.83%	3b
2021 ⁷⁷	ML Supervised ML; SVM; KNN; X Boost; LR	DI system classification	PR	Classification accuracy Hu values: SVM 0.47, KNN 0.33, LR 0.50, X Boost 0.33 Classification accuracy eigenvalues: SVM 0.67, KNN 0.17, LR 0.67, X Boost 0.67	3b
2021 ⁷⁸	DL ResNet 18, 34, 50, 101, 152 (single; multi-task)	DI system classification	9767 PR	Best: multi-task accuracy (0.9803–0.9908), recall (0.9727–0.9886), AUC-ROC (0.9997–0.9999) Best accuracy: ResNet152 in implant classification (0.9908), in treatment stage (0.9972)	3b
2022 ⁷⁹	DL EfficientNet-B0; EfficientNet-B4; Meta Pseudo Labels 1; Meta Pseudo Labels 2	Classification of 79 DI types	45,396 PR	Top–1 accuracy: EfficientNet-B0 (89.4), EfficientNet-B4 (89.4), Meta Pseudo Labels 1 (87.96), Meta Pseudo Labels 2 (88.35) Top–5 accuracy: Meta Pseudo Labels 1 (97.90), Meta Pseudo Labels 2 (97.79)	3b
2022 ⁸⁰	DL FCN-1, FCN-2	DI system classification	483 2D virtual images	Virtual X-ray accuracy: 98% Precision, recall, accuracy, F1: Set 1: 74.38%, 90.98%, 90.43%, 80.73% Set 2: 68.31%, 78.64%, 94.06%, 84.48% Human, Set 1: 70.52%, 69.76%, 69.76%, 69.70% Human, Set 2: 70.55%, 68.67%, 68.67%, 67.60% Pig X-ray, Set 1: 73.04%, 74.63%, 74.63%, 72.23% Pig X-ray, Set 2: 73.12%, 71.72%, 71.72%, 70.75%	3b
2022 ⁸¹	DL ResNet50-v2, Xception, VGG16	DI system classification	PA	Training accuracy; testing accuracy: Xception (75%; 93%); ResNet50-v2 (81.25%; 100%); VGG16 (75%; 93%)	3b
2022 ⁸²	DL ResNet 18, 50, 152	DI system classification	10,191 PR	ResNet18: AUC-ROC 0.9993	3b
2022 ⁸³	DL YOLOv3	DI system classification	263 PA	Sensitivity, specificity, accuracy, confidence score: 94.4%, 97.9%, 96.7%, 0.75	3b

Table 2F. (Continued)

Year Ref.	Technology AI model	Purpose	Data	Results	OEL
2023 ⁸⁴	DL Custom DL engine (NeutoT)	DI system classification	156,965 PA + PR	Best performance in bone level implant classification: sensitivity, specificity, accuracy 100% Accuracy, precision, recall, F1: Total: 88.53%, 85.70%, 82.30%, 84% PR: 87.89%, 85.20%, 81.10%, 83.10% PA: 86.87%, 84.40%, 81.7%, 83.00%, 83%	3b
2023 ⁸⁵	DL Google AutoML Vision	DI system classification	4800 PA	Accuracy 0.981, precision 0.963, recall 0.961, specificity 0.985, F1 0.962	3b
2023 ⁸⁶	DL, ML VGG16; k-means	DI diameter and length classification	1320 PA	VGG16: accuracy (0.994), sensitivity (0.950), specificity (0.994), F1 (0.974), PPV (0.952), NPV (0.975) k-means: accuracy (0.983), sensitivity (0.900), specificity (0.988), F1 (0.923), PPV (0.909), NPV (0.988)	3b
2023 ⁸⁷	DL VGG16; VGG19; ResNet50; ResNet101; GoogLeNet, Fusion	DI system classification	11,904 PR	Accuracy; F1 per implant type; sensitivity per implant type; specificity per implant type: VGG16: 97.6; (96.2, 96.8, 99, 98.1, 98.3); (98, 96.6, 98.9, 98.2, 97.8); (99.6, 99.5, 99.2, 99.6, 99.7) VGG19: 98.3; (96, 97.4, 99, 98.2, 98.5); (98.4, 96.8, 98.9, 98.5, 98.3); (99.6, 99.6, 99.3, 99.6, 99.7) ResNet50: 97.9; (95.1, 96.7, 99, 97.9, 97.6); (96.1, 95.9, 99, 98.2, 97.6); (99.6, 99.5, 99, 99.6, 99.5) ResNet101: 98.1; (95.1, 96.7, 99, 97.9, 97.6); (95.4, 96, 99, 98.3, 98.5); (99.6, 99.6, 99, 99.6, 99.6) GoogLeNet: 97.2; (93.7, 95.3, 98.5, 97.3, 97.1); (94.9, 94.1, 98.7, 98, 96.7); (99.5, 99.4, 98.7, 99.4, 99.4) Fusion: 98.9; (97.4, 98, 99.3, 99.9, 99.1); (99.2, 97.1, 99.4, 99.1, 98.9); (99.7, 99.8, 99.4, 99.8, 99.8)	3b
2023 ⁸⁸	DL Ensemble, EfficientNet, Res2Next	Classification of 130 DI types	45,909 PR	Ensemble: top-1 accuracy 75.27%, top-5 accuracy 95.02%, precision 78.84%, recall 75.27%, F1 74.89%	3b
2023 ⁸⁹	DL ResNet50	DI system classification	150,733 PA + PR	Total: accuracy (82.3%), AUC-ROC (0.823), sensitivity (80.0%), specificity (84.5%), PPV (83.8%), NPV (80.9%) PA: accuracy (83.8%), AUC-ROC (0.838), sensitivity (81.5%), specificity (86%), PPV (85.3%), NPV (82.3%) PR: accuracy (73.3%), AUC-ROC (0.733), sensitivity (71.5%), specificity (75%), PPV (74.1%), NPV (72.5%)	3b
2023 ⁹⁰	DL YOLOv5; YOLOv7	Classification of 103 DI types	14,037 PR	mAP: YOLOv5 (0.973), YOLOv7 (0.988)	3b
2023 ⁹¹	DL VGG16	DI system classification	1390 PA	Training loss: 0.0037; accuracy: 1	3b
2024 ⁹²	DL ConvNeXt, RegNet, DenseNet, EfficientNet, VGG, Swin Transformer, ViT	DI system classification	1258 PR	Best: ConvNeXt with accuracy 94.2%, precision 95.6%, recall 93.3%, F1 94.2%	3b
2024 ⁹³	DL ConvNeXt, VGG16, ResNet50, Vovnet57a, EfficientNet, MobileNet, ViT, Swin Transformer	DI system classification	1258 PR	Best: ConvNeXt with accuracy 95.74%, precision 96.01%, recall 94.72%, F1 95.22%	3b
2023 ⁹⁴	DL YOLOv8m-seg	DI system classification	2573 PA	Precision 0.919, recall 0.98, F1 0.95, mAP 0.972	3b
2024 ⁹⁵	DL ResNet50	DI system classification	157,495 PA + PR	Accuracy 95.05%, precision 95.91%, recall 92.49%, F1 94.17%	3b
2024 ⁹⁶	DL YOLOv7; EfficientNet	DI system classification	1574 PR	Recall; precision; F1; accuracy: YOLOv7: 1; 0.979; 0.989; 0.989 EfficientNet: 0.917-1; 0.978-1; 0.941-1; 0.952-1	3b
2023 ⁹⁷	DL GoogLeNet, Inception-ResNet152-v2, Inception-v3, ResNet 50, 50V2, 101, 101V2, 152, 152V2	DI system classification	13,500 2D CBCT (in vitro)	Training accuracy; test accuracy; AUC-ROC: GoogLeNet (1; 0.983; 1) Inception-ResNet152-v2 (0.993; 0.975; 1) Inception-v3 (0.893; 0.948; 1) ResNet50 (0.992; 0.854; 1) ResNet50V2 (0.991; 0.925; 1) ResNet101 (0.995; 0.807; 1)	3b

Table 2F. (Continued)

Year Ref.	Technology AI model	Purpose	Data	Results	OEL
				ResNet101V2 (0.994; 0.936; 1)	
				ResNet152 (0.995; 0.932; 1)	
				ResNet152V2 (0.989; 0.993; 1)	

2D, two-dimensional; 95% CI, 95% confidence interval; AP, average precision; AUC-ROC, area under the receiver operating characteristic curve; CBCT, cone beam computed tomography; CNN, convolutional neural network; DCNN, deep convolutional neural network; DI, dental implant; DL, deep learning; F1, F1 score; KNN, k-nearest neighbours; LR, logistic regression; mAP, mean average precision; mIoU, mean intersection over union; ML, machine learning; NBS, Nobel Brånemark System; NNA, Nobel NobelActive; NPV, negative predictive value; OEL, Oxford Centre for Evidence-Based Medicine level of evidence; PA, peri-apical radiograph; PPV, positive predictive value; PR, panoramic radiograph; SBL, Straumann bone level; STL, Straumann tissue level; TP, true positive; YI, Youden index; ZSP, Zimmer SwissPlus; ZTSV, Zimmer Biomet Dental Tapered Screw-Vent.

Naïve Bayes ($n = 4$)

Naïve Bayes is a probabilistic algorithm based on Bayes' theorem, proposed by Lewis in 1998¹⁴⁴. It assumes that the features of a data point are independent given its class, which allows for fast and efficient training and classification¹⁴⁴. Three of the four studies using naïve Bayes used structured data as input (75%), while the other study used 2D images (25%). The average number of data samples was 362.7.

k-nearest neighbours (KNN) ($n = 3$)

KNN is a non-parametric and instance-based learning algorithm proposed by Evelyn Fix and Joseph Hodges in 1951¹⁴⁵. KNN classifies new data points by finding the k-nearest neighbours in the training set and assigning the class label based on the majority vote¹⁴⁵. One (33.3%) of the three studies using KNN used structured data as input, while two (66.7%) used 2D images. The average number of data samples was 660.

Decision tree ($n = 3$)

Decision tree is a tree-based model for supervised classification and regression tasks. It consists of a tree structure where each node represents a feature or attribute, and each edge represents a decision or rule. Decision tree recursively splits the data into subsets based on the feature values and assigns a class label or a numerical value to each leaf node. Two (66.7%) of the three studies using a decision tree used structured data as input, while one (33.3%) used

2D images. The average number of data samples was 283.3.

MobileNet ($n = 6$)

MobileNet is a lightweight CNN architecture designed for efficient image processing on mobile devices. It utilizes depthwise separable convolutions to achieve a good balance between computational efficiency and high accuracy in tasks such as image classification¹⁴⁶. All of the studies using MobileNet employed images as input data (83.3% of them in 2D and 16.7% in 3D), with an average number of images of 3319.

EfficientNet ($n = 6$)

EfficientNet is a state-of-the-art CNN architecture designed to optimize model efficiency and accuracy through a novel compound scaling method. EfficientNet achieves superior performance by scaling the network's depth, width, and resolution simultaneously. This approach ensures a well-balanced trade-off between computational efficiency and model accuracy across a wide range of tasks¹⁴⁷. All of the studies using EfficientNet employed images in 2D as input data, to test and validate it, with an average number of images of 16,126.8.

AlexNet ($n = 4$)

AlexNet is a seminal deep CNN architecture that has played a pivotal role in advancing image classification tasks¹⁴⁸. Notable for its deep architecture and introduction of the rectified linear unit (ReLU) activation function, AlexNet demonstrated superior performance in

the ImageNet Large Scale Visual Recognition Challenge, marking a significant milestone in the field of deep learning. All of the studies using AlexNet employed images in 2D as input data, with an average number of images of 4290.5.

DenseNet ($n = 3$)

DenseNet, or densely connected convolutional network, is a deep learning architecture where each layer is directly connected to every other layer in a feed-forward manner. It promotes feature reuse, reduces the number of parameters, and mitigates the vanishing gradient problem, leading to more efficient and accurate models. DenseNet has shown strong performance in image classification and segmentation tasks¹⁴⁹. Only 2D images were used in these studies, with an average number of images of 1825.7.

Xception ($n = 3$)

Xception is a deep convolutional neural network architecture that leverages depthwise separable convolutions to improve efficiency and performance. This design reduces computational complexity by factorizing standard convolutions into spatial and depthwise operations, allowing for a more precise extraction of spatial features¹⁵⁰. Only 2D images were used in these studies, with an average number of 7681.5 images.

Outcomes and metrics of the studies

The studies included in this review reported a variety of results, the success

Table 2G. Key characteristics of the studies in the 'implant planning' group.

Year Ref.	Technology AI model	Purpose	Data	Results	OEL
2021 ⁹⁸	DL Software: Diagnocat	Detection of structures and bone dimension calculation with a commercial software compared to professionals	CBCT	Kolmogorov–Smirnov test for normality Detection: canals 72.2%, sinuses/fossae 66.4%, missing teeth 95.3% (484/508 correct) AI failures: 80 bone height, 15 bone thickness measurements Bone height: no significant AI–manual differences (premolars, $P > 0.05$) Bone thickness: significant AI–manual differences (all regions, $P < 0.001$)	3b
2021 ⁹⁹	DL ResNeXt101	Immediate implant placement AI tool through sagittal root inclination measurements	4144 2D CBCT	Error: 2.16°, correlation: 0.915 (manual) Bland–Altman CI: narrow Manual vs model difference: $0.16 \pm 2.95^\circ$	3b
2021 ¹⁰⁰	DL Faster R-CNN	Learning curve of the AI for dental implant planning in the posterior maxillary region Identification of the implant to be placed	316 2D CBCT	Panoramic detection: original 62.5%, blurred 75%, sharpened 43.75%, coloured 31.25%, noise 50% Cross-sectional detection (300 images): original 62.5%, blurred 75%, sharpened 62.5%, coloured 56.25%, noise 50% Panoramic accuracy: original 60%, blurred 41.66%, sharpened 71.42%, coloured 100%, noise 62.50% Cross-sectional accuracy: original 70%, blurred 50%, sharpened 80%, coloured 88.89%, noise 87.50%	3b
2022 ¹⁰¹	DL Mask R-CNN; Faster R-CNN; ResNet101	Tooth instance segmentation and detection of missing tooth regions	455 PR	Segmentation: mAP50, 92.14%; mAP50-95, 76.78% Detection: mAP50, 59.09%; mAP50-95, 20.40%	3b
2022 ¹⁰²	DL U-Net	Detection and classification of oral structures	800 2D CT	Total: accuracy (92.39%); precision (92.35%); sensitivity (93.48%); specificity (92.07%).	3b
2022 ¹⁰³	DL Mask R-CNN	Position of radiographic stent gutta percha markers	30 CBCT	AI true positive rate: 83% (GP markers) False positives: 28% mislabelled as GP, overall rate 2.8%	3b
2024 ¹⁰⁴	DL MobileNet	Identify implant–ridge relationship	630 CBCT slices	Accuracy: A (0.84), B (0.9528), C (0.9528)	3b
2023 ¹⁰⁵	DL U-Net	Edentulous alveolar bone segmentation	43 CBCT	DSC: training (0.89), testing (0.78), total (0.83)	3b
2023 ¹⁰⁶	DL SinusC-Net	Implant procedure selection according to sinus condition	133 CBCT	Mean: accuracy (0.97), sensitivity (0.92), specificity (0.98), AUC-ROC (0.95)	3b
2023 ¹⁰⁷	DL TCEIP (ResNet)	Predict implant position	3045 CBCT slices	AP75: 17.8	3b
2024 ¹⁰⁸	DL YOLOv7; YOLOv7-X; YOLOv7-W6; MSPENet	Predict implant position	3045 CBCT slices	Object detection: YOLOv7 (precision: 0.781; recall: 0.845; AP75: 0.84; FPS: 72) YOLOv7-X (precision: 0.869; recall: 0.815; AP75: 0.878; FPS: 65) YOLOv7-W6 (precision: 0.868; recall: 0.842; AP75: 0.893; FPS: 57)	3b
2020 ¹⁰⁹	DL U-Net, Dense Block, Spatial Dropout	3D tooth segmentation	102 CBCT	Validation: Dice 0.938, recall 0.952, precision 0.924 Test: Dice 0.918, recall 0.932, precision 0.904	3b
2024 ¹¹⁰	DL U-Net	Segment bone in missing teeth regions and predict implant position	150 CBCT	Bone segmentation: Dice 0.81, Jaccard 0.68, precision 0.87, recall 0.75, volume error rate 14.32% ROI: Dice 0.93, Jaccard 0.88, precision 0.94, recall 0.93, volume error rate 1%	3b
2024 ¹¹¹	DL Software: Relu Creator	CBCT and IOS registration compared to manual and semi-automated	31 CBCT and IOS	MSD: 0.04 mm, RMS: 0.19 mm (AI higher accuracy and efficiency over manual and semi-automated)	3b
2024 ¹¹²	DL TPNet with ResNet50; 2D/3D ResBlocks	Implant depth prediction	400 CBCT	Acc(R@1, IoU = m): IoU = 0.6: 33.9%; IoU = 0.7: 25.4%; IoU = 0.8: 20.3%	3b

2D, two-dimensional; 3D, three-dimensional; Acc(R@1, IoU = m), accuracy of top-1 predicted moments whose IoU with the ground-truth moment is larger than m; AP75, average precision at IoU = 0.75; AUC-ROC, area under the receiver operating characteristic curve; CBCT, cone beam computed tomography; CI, confidence interval; CT, computed tomography; DL, deep learning; DSC, Dice similarity coefficient; F1, F1 score; FPS, frames per second; IOS, intraoral scan; IoU, intersection over union; mAP50, mean average precision at an IoU threshold of 0.50; mAP50-95, average of the mean average precision calculated at varying IoU thresholds ranging from 0.50 to 0.95; MSD, median surface deviation; OEL, Oxford Centre for Evidence-Based Medicine level of evidence; PR, panoramic radiograph; RMS, root mean square; ROI, region of interest.

Table 2H. Key characteristics of the studies in the 'implant prognosis' group.

Year Ref.	Technology AI model	Purpose	Data	Results	OEL
2018 ¹¹³	ML DT; SVM	Predict key factors for implant prognosis	59 SD	Most significant factor: mesiodistal position (accuracy 0.93)	3b
2018 ¹¹⁴	ML C4.5 DT, LR, SVM with/without Bagging or AB	Predict implant failure	747 SD	(Accuracy; sensitivity; specificity; AUC-ROC): DT (0.68; 0.59; 0.77; 0.67) LR (0.62; 0.61; 0.64; 0.64) SVM (0.63; 0.58; 0.82; 0.74) Bagging + DT (0.70; 0.58; 0.82; 0.74) Bagging + LR (0.63; 0.57; 0.68; 0.67) Bagging + SVM (0.62; 0.60; 0.64; 0.67) AB + DT (0.67; 0.47; 0.87; 0.74) AB + LR (0.60; 0.51; 0.69; 0.66) AB + SVM (0.63; 0.51; 0.75; 0.65)	3b
2022 ¹¹⁵	DL NN	Single implant survival prediction	1626 SD	Accuracy: 94.45%; F1 score: 0.9657; recall: 0.9837; specificity: 0.9565	3b
2022 ¹¹⁶	ML and DL LR, VGG16, IM	Dental implant loss risk	680 2D CBCT	IM (AUC-ROC = 0.90, 95% CI 0.84–0.95) DL (AUC-ROC = 0.87, 95% CI 0.80–0.92) LR (AUC-ROC = 0.72, 95% CI 0.63–0.79)	3b
2023 ¹¹⁷	DL ResNet50	Implant outcome prediction	1080 PR + PA	(Accuracy; precision; recall; F1) Hybrid model: (0.870; 0.85; 0.88; 0.85) Only PA: (0.786; 0.84; 0.73; 0.75) Only PR: (0.787; 0.87; 0.63; 0.66)	3b
2023 ¹¹⁸	DL ResNet 18, 34, 50; DenseNet 121, 201; MobileNet-v2, v3	Predict osseo-integration of dental implants	1206 PR + PA	(Accuracy; specificity; sensitivity) ResNet18: (0.806; 0.802; 0.811) ResNet34: (0.822; 0.810; 0.832) ResNet50: (0.836; 0.857; 0.817) DenseNet121: (0.818; 0.813; 0.823) DenseNet201: (0.816; 0.809; 0.827) MobileNet-v2: (0.824; 0.816; 0.833) MobileNet-v3:(0.799; 0.780; 0.819)	3b
2024 ¹¹⁹	ML Two-step clustering, Cox regression, Kaplan–Meier	Predict implant loss risk	8513 SD	High risk factors: age, smoking history, implant diameter, implant length, implant position and surgical procedure Concordance index: 0.642 (0–120 days), 0.781 (120–310 days), 0.715 (> 310 days)	2b
2024 ¹²⁰	DL	Implant success prediction	150 CBCT	Traditional accuracy 78%; AI accuracy 87%	2b
2024 ¹²¹	DL ResNet50	Identify ridge deficiencies around implants	1475 CBCT slices	Mandible: accuracy 98.91%, F1 97.30% Maxilla: accuracy 98.82%, F1 95.86%	3b
2020 ¹²²	ML SVM, ANN, LR, RF	Predict severe MBL with implants	81 SD	(AUC-ROC; sensitivity; specificity) SVM (0.967; 91.67%; 100.00%) ANN (0.928; 91.67%; 93.33%) LR (0.906; 91.67%; 93.33%) RF (0.842; 75.00%; 86.67%)	3b
2021 ¹²³	DL Mask R-CNN; ResNet	Implant detection Upper/lower jaw and bone loss classification	708 PA	Models mean OKS: upper 0.8748, lower 0.9029, total 0.8885 Dentists mean OKS: total 0.9012	3b
2022 ¹²⁴	DL Faster R-CNN: Inception-ResNet-v2	Marginal bone loss sites and implant detection	835 PA	Bone loss/lesions: PPV 81%/87%, sensitivity 67%/75%, specificity 87%/83% AI-expert: $\kappa = 0.547/0.568$ (bone loss/implants) Dentist: $\kappa = 0.555/0.544$ (bone loss/implants)	3b
2023 ¹²⁵	ML NB, RF, GB, LR, KNN, DT, SVM, CN2 Rule Inducer	Prediction of physiological bone remodelling	44 PA	(AUC-ROC, 95% CI, sensitivity, specificity, PPV, NPV) NB (0.75, 0.65–0.85, 66%, 68.4%, 73.3%, 60.5%) RF (0.69, 0.58–0.80, 70%, 55.3%, 67.3%, 58.3%) GB (0.65, 0.53–0.77, 60%, 57.9%, 56.6%, 41.7%) LR (0.65, 0.53–0.77, 46.1%, 71.1%, 67.6%, 50%) KNN (0.64, 0.52–0.76, 62%, 65.8%, 70.5%, 56.8%) DT (0.57, 0.32–0.55, 66%, 44.7%, 61.1%, 50%) SVM (0.37, 0.24–0.49, 68%, 27.3%, 54.8%, 38.5%) CN2 (0.27, 0.16–0.39, 86%, 13.3%, 56.6%, 41.6%)	3b
2023 ¹²⁶	DL U-Net; Otsu thresholding		50 3D XRT	Accuracy: 87%	3b

Table 2H. (Continued)

Year Ref.	Technology AI model	Purpose	Data	Results	OEL
2021 ¹²⁷	ML Hierarchical clustering; NB	Collagen fibres and bundles segmentation in peri-implant tissue Peri-implantitis classification by immune profile, microbes Predict outcomes	24 SD	Unsupervised clustering: risk groups Low-risk: high M1/M2, low B-cells, complement signalling, Th1/Th17 High-risk: <i>Fusobacterium nucleatum</i> , <i>Prevotella intermedia</i> Surgery reduced microbes; re-colonization suppressed only in low risk	3b
2021 ¹²⁸	ML LR, SVM, RF	Predict peri-implantitis	1408 SD	Highest performance: RF (AUC-ROC: 0.71, accuracy: 0.70, precision: 0.72, recall: 0.66, F1: 0.69)	3b
2024 ¹²⁹	DL YOLOv7	Peri-implantitis and marginal bone loss classification	800 PA	Accuracy 94.74%, sensitivity 94.44%, specificity 100%, precision 100%, recall 94.44%, F1 97.10%	3b
2022 ¹³⁰	ML NB, RF, AB, improved AB	Predict the need for dental implants	107 SD	Accuracy: NB (72.8%), RF (77.8%), AB (86.1%), improved AB (91.7%)	3b
2022 ¹³¹	DL MobilenetV2-DeeplabV3+; ResNet50	Implant stability classification	779 CBCT	Implant segmentation: mIoU (0.944), PxA (0.968), recall (0.969), precision (0.973) Implant stability: (sensitivity, specificity, PPV, NPV, F1) class 0–49 (0.93, 1.0, 1.0, 0.98, 0.96); class 50–59 (0.96, 0.99, 0.93, 0.99, 0.95); class 60–70 (0.92, 0.98, 0.96, 0.96, 0.94); class 70–100 (0.96, 0.95, 0.90, 0.95, 0.93)	3b
2022 ¹³²	ML Multivariate linear regression	Predict postoperative discomfort	1032 SD	Root mean square error: 0.1085; accuracy: 89.6%	3b
2023 ¹³³	ML GB, distributed RF, XGBoost, stacked ensemble, generalized linear model, DL	Predict medication osteonecrosis risk in dental extraction/ implantation patients	340 SD	AUC-ROC 0.8283 (training), 0.7526 (test); best model: GB	3b

2D, two-dimensional; 3D, three-dimensional; AB, AdaBoost; ANN, artificial neural network; AUC-ROC, area under the receiver operating characteristic curve; CBCT, cone beam computed tomography; 95% CI, 95% confidence interval; DL, deep learning; DT, decision tree; F1, F1 score; GB, gradient boosting; IM, integrated model; KNN, k-nearest neighbours; LR, logistic regression; MBL, marginal bone loss; mIoU, mean intersection over union; ML, machine learning; NB, naïve Bayes; NN, neural network; NPV, negative predictive value; OEL, Oxford Centre for Evidence-Based Medicine level of evidence; OKS, object keypoint similarity; PxA, pixel accuracy; PA, peri-apical radiograph; PPV, positive predictive value; PR, panoramic radiograph; RF, random forest; SD, structured data; SVM, support vector machine; XRT, X-ray tomography.

being reflected in the metrics of each study.

Performance metrics calculated in each study varied, making it difficult to compare results. Some metrics were used in several studies, including accuracy, precision, F1 score, area under the receiver operating characteristic curve (AUC-ROC), sensitivity, specificity, recall, Pearson correlation coefficient (r), Dice similarity coefficient (DSC), intersection over union (IoU), and mean average precision at an IoU threshold of 0.50 (mAP50). However, the metrics also depend on the nature of the problem and result, and some metrics only apply to classification problems (e.g., sensitivity, specificity, precision, recall).

All performance metrics provided were calculated from in silico validation studies, where some data were kept for validation of the algorithms.

Just over half (56.7%) of the studies focused primarily on image classification, encompassing diverse types of implants, various bone structures, and distinct oral structures. These studies commonly employed key metrics, facilitating comparability. The four most frequently utilized metrics in these studies were accuracy, precision, F1 score, and recall.

Fig. 4 shows bar and whisker graphs representing these metrics for the different topics. Instances exist where a single article computed multiple algorithms, yielding varying results; the outcomes of all evaluated algorithms are presented herein. It is noteworthy that the efficacy of each study's performance hinged significantly on the quantity of images used in training and the diversity of types to be classified.

All studies that focused on implant classification, except two, reported

accuracy as a metric. These studies achieved accuracy, AUC-ROC, recall, and F1 score rates above 81%, except for two studies^{77,88}, demonstrating the consistently high performance in this area. Similarly, studies addressing the segmentation of various dental structures for diagnosis, structure classification, restoration classification, and implant planning, reported accuracy rates exceeding 83%, AUC-ROC values above 92%, and Dice values above 93%, except for two studies^{51,98}.

Studies that focused on bone classification also showed excellent results, with all reporting accuracy values above 98%, precision over 96%, and F1 scores exceeding 96%. Articles discussing guided surgery applications also demonstrated accuracies above 94% and precision values above 87%.

However, in other applications, such as prognosis, the results were somewhat

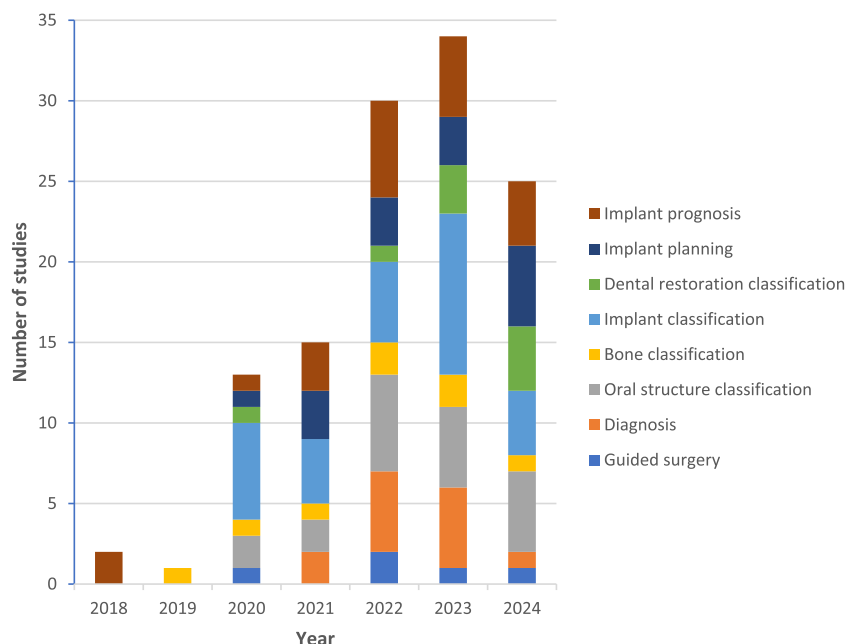


Fig. 2. Number of studies per year of publication and according to the topic categories.

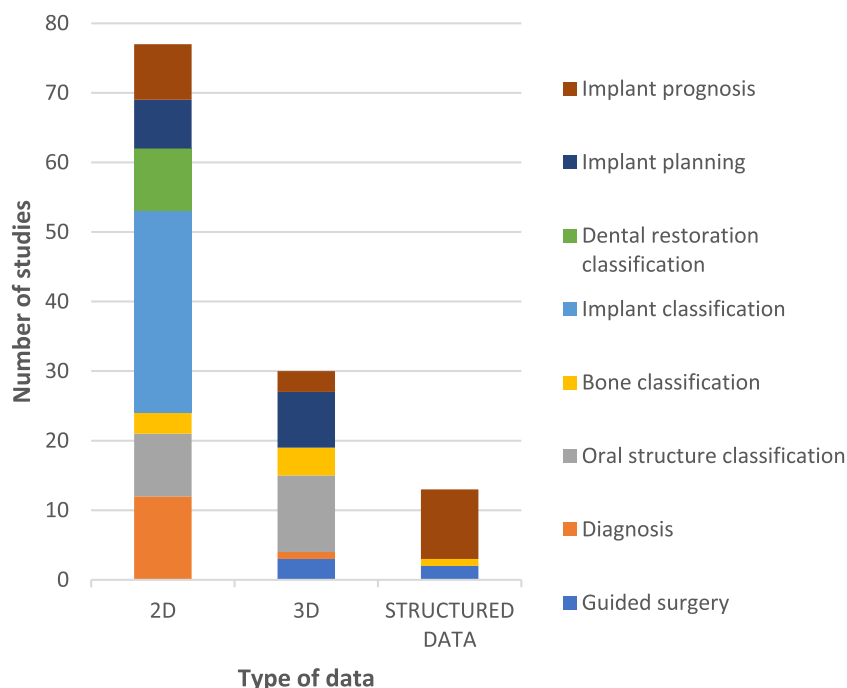


Fig. 3. Number of studies per type of data used and according to the topic categories.

lower, with accuracy values exceeding 70%. Nonetheless, some studies reported accuracy rates as high as 99.7%, precision of 97.3%, and recall of 96.8%, depending on the specific objectives of the research.

Risk of bias

Supplementary material Table S1 shows the risk of bias analysis of the

studies. Eleven studies showed a high risk of bias and five had an unclear risk of bias. The remaining studies were considered to have a low risk of bias.

OCEBM level of evidence

With the exception of three studies classified as 2b^{14,119,120} and one as 3a⁵³, the remaining articles were classified as OCEBM evidence level 3b. This

classification reflects the fact that they describe technical studies of diagnostic validation. Although clinical images or data were used, these studies did not involve direct clinical intervention in patients, nor were any of them randomized controlled trials. Consequently, they are positioned at a lower level within the OCEBM evidence hierarchy, which is primarily designed for the assessment of clinical interventions in humans.

Origins of the studies

The analysis showed that 28 of the 120 studies (23.3%) were conducted in South Korea, 24 (20%) in China, nine (7.5%) in Turkey, eight (6.7%) in each of Japan and India, six (5%) in Taiwan, and five (4.2%) in Saudi Arabia. Among the remaining studies ($n = 32$), fewer than five were conducted in any one country.

Discussion

This review of 120 studies on AI in implantology highlights a powerful shift in the field. The studies, predominantly using deep learning algorithms like ResNet and U-Net, investigated various aspects of implantology, from guided surgery to prognosis. The surge in publications, especially focusing on 2D radiographs, reflects a dynamic evolution in recent years. Despite the varying performance metrics, of which accuracy, precision, F1 score, and recall were the most frequently utilized, most studies demonstrated a low risk of bias. This review underscores the growing influence of AI, particularly deep learning, in shaping the future of implantology, highlighting the imperative for standardized reporting and metrics in this transformative arena.

Topic

The implementation of AI in implant dentistry is still in its nascent stages, presenting abundant opportunities for further advancement and improvement in various areas. Nevertheless, there have been rapid developments in recent times, with a particular focus on guided surgery, diagnosis, classification of oral structures, and bone and dental restorations, as well as implant identification, planning, and prognosis. These advancements predominantly rely on the integration of imaging techniques and

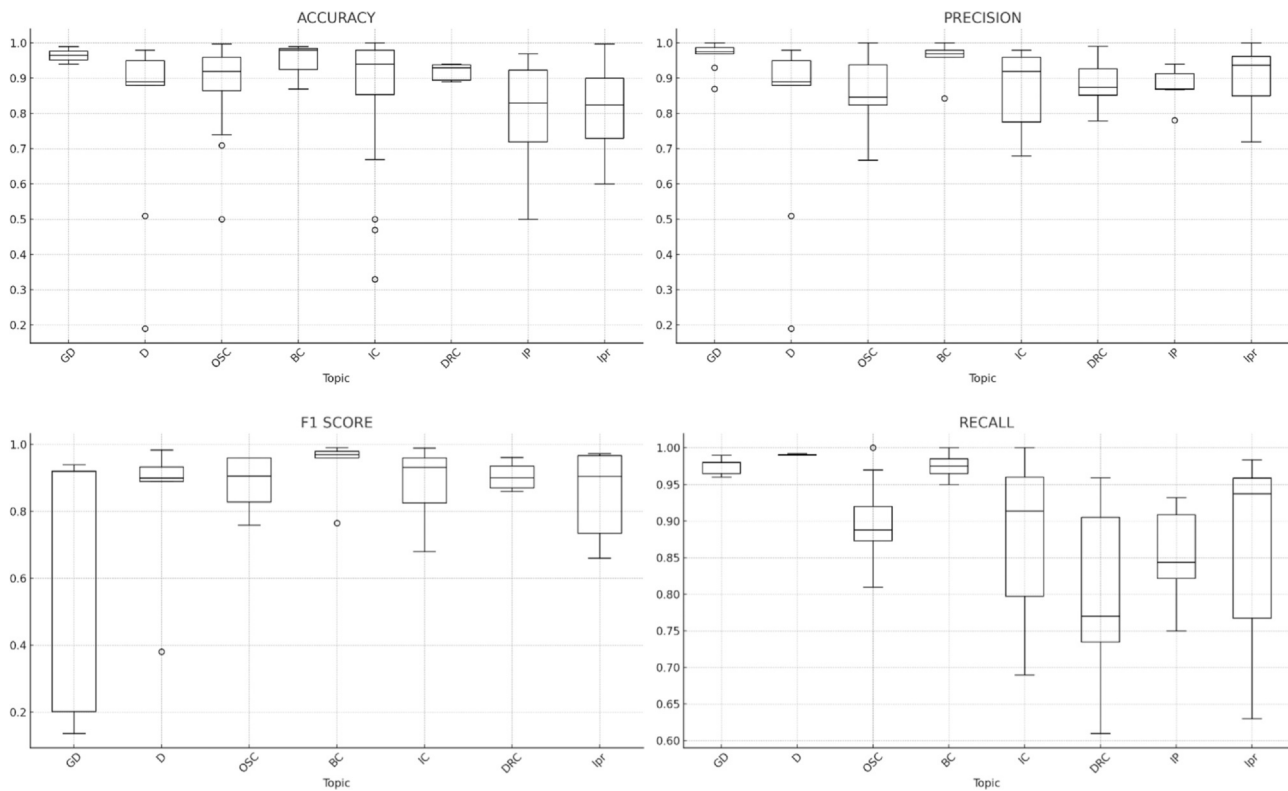


Fig. 4. Metrics—accuracy, precision, F1 score, recall. GD, guided surgery; D, diagnosis; OSC, oral structure classification; BC, bone classification; IC, implant classification; DRC, dental restoration classification; IP, implant planning; IPr, implant prognosis.

deep learning algorithms, highlighting the significance of this combination in driving progress within the field.

Type of data

When considering the types of data handled in the implantology sector, three areas of interest can be identified as potential focuses for further efforts: searching for and identifying various types of information in radiographs, whether in 2D or 3D, and in images from intraoral scanners; extracting information from medical records; and using AI for the design and manufacturing of personalized or generic dental implants and prostheses.

Regarding images, areas of particular interest for future studies are the classification of all types of structures, detection and categorization of diseases, and classification of bone structures and bone quality in images. Most of the studies to date have focused on 2D images, but the use of the same technology for 3D images is a field to be explored. The identification and classification of dental implants was the most represented topic (29 studies, 24.2%). However, all of the studies in this group used 2D images. Only one

claimed to use 3D images, but then transformed the images to 2D. The absence of implant classification in 3D images is particularly striking, and this seems to be a promising field for computer-aided odontology software.

The use of images as data predominated in the field of dental implantology, with 89.2% of the studies using this type of data. Although structured data were only used in 10.8% of the studies, the use of AI applied to dental implant medical records is expected to become more important in the coming years, especially as these databases become better annotated and more complete.

Technology employed

Certain algorithms have demonstrated superior suitability and have consequently been exclusively used in studies involving images. Examples of such algorithms include ResNet, U-Net, R-CNN, GoogLeNet, VGG, YOLO, MobileNet, EfficientNet, AlexNet, DenseNet, and Xception. However, it is worth noting that none of the algorithms employed in more than two studies were exclusively used for handling structured data. This observation

can be attributed to the fact that a significant majority (89.2%) of the studies focused on image data. As a result, many studies within the field have compared different algorithms to assess their performance in the context of implant dentistry. This comparison is relevant even if a particular algorithm may not be the optimal choice for a specific case. Such comparisons offer valuable insights into the strengths and limitations of various popular algorithms, informing researchers and practitioners about their potential applications in the field.

Quantity of data samples

The variation in the number of data points from study to study is quite significant, ranging from as low as 20 to as high as 157,495 for image data, and from 24 to 8513 for structured data. This discrepancy primarily stems from the fact that the availability of data has been a more influential factor in determining the sample size in most cases, rather than adhering to an ideal amount for development of the algorithm.

In the domain of structured data, a thorough observation reveals gaps in a substantial portion of patient

information, creating the initial illusion of data abundance that, in reality, has not been adequately stored, resulting in incomplete datasets. To address this issue, efforts are being directed towards enhancing the precise storage of information. This push towards more effective data management aligns with the ongoing digitization of systems, contributing to heightened integrity and quality in preserving clinical data.

Concerning imaging, the task of labelling poses a considerable challenge in terms of time and resources in most cases. This circumstance often leads to the selective use of efficiently processable raw data, despite the availability of ample data. Moreover, the computational cost tied to image training significantly surpasses that of structured data, necessitating increased processing power as more images come into play. This consideration gains even more relevance and complexity when dealing with 3D images.

Risk of bias

Two key factors emerged as the most common reasons for a 'high risk' classification. Firstly, the separation of test and training data was often not appropriately executed, leading to potential overfitting or inadequate model generalization. Secondly, many studies failed to comprehensively analyse all of the variables that could potentially influence the problem under investigation. For instance, some studies converted 3D images to 2D and used different parts of the same image for both testing and training, compromising the validity of the results.

Additionally, in studies involving structured data, a frequent issue pertained to the mishandling or lack of information regarding missing and/or erroneous values, impacting the accuracy and reliability of the findings.

Moreover, it is important to note that AI content in software and industrial products is not always explicitly declared. This lack of transparency raises concerns, particularly when applications do not behave predictably or uniformly, leading to suspicion that they may contain AI components. In the context of medical devices, such as ultrasound sonography or CBCT, this uncertainty emphasizes the need for clinicians to use these tools with caution. The doctor must verify the plausibility of the results to ensure safe and accurate patient care.

Limitations

This review has certain limitations, particularly the potential exclusion of studies relevant to implant dentistry, such as those focusing on the identification of structures like the dental nerve, if they did not explicitly mention 'implant dentistry' in their titles or abstracts. In addition, some of the articles could not be obtained for review. This aspect could have led to valuable research being overlooked that could contribute to the field. Moreover, the heterogeneity of the articles, as well as of the training data and algorithms used, makes it challenging to compare the results across studies.

When analysing the data, it became evident that the results of the common metrics were highly disparate, as they depended not only on the algorithm and objective but also on the quality and quantity of the data. In fact, some studies concluded that their path to improvement consists of increasing the amount of training data⁷⁷.

To address these limitations and further expand the scope of relevant studies, future research endeavours could involve extending the search to specific areas of interest within implant dentistry, even if the term 'implantology' is not explicitly used. By incorporating relevant keywords and synonyms related to specific implant dentistry topics, a more comprehensive and inclusive examination of the literature can be achieved.

Future perspectives

Anticipated future developments in this field might encompass the incorporation of 3D imaging for implant type classification. This trend is expected to emerge alongside the widespread adoption of 3D CBCT scanners, which hold the potential to revolutionize and augment implant planning and diagnostics. By integrating high-quality 3D imaging data, AI algorithms could offer more precise and personalized implant classification, contributing to improved treatment outcomes and patient care.

Conclusions

In conclusion, the predominant focus of the current literature centres on the development of AI algorithms tailored for the 2D classification of dental implants, with common applications extending to the identification of

structures such as teeth, maxillary sinus, and dental nerves.

The ability of AI to identify implant types in 2D medical images already surpasses the accuracy of practitioners^{69,76}, offering a valuable tool that does not require clinicians to recognize commercial brands of implants they may not have encountered before. However, expanding the range of implants that can be identified is essential to maximize the utility of this application.

The studies on segmentation of dental structures for diagnosis, classification, restoration, and implant planning have demonstrated consistently high performance, with accuracy rates exceeding 83%, AUC-ROC values above 92%, and DICE values above 93%. While these results indicate that AI has the potential to enhance clinical workflows, this use of AI serves primarily as a visual aid to professionals rather than making decisions autonomously. As such, it can be implemented even with some degree of error. Indeed, several existing software programs already incorporate AI for these applications, although there is still scope for improvement, particularly in refining algorithms for more complex cases.

For bone classification, the outcomes were particularly impressive, with all studies reporting accuracy, precision, and F1 scores above 96%. These high levels of performance demonstrate the robustness of AI in this specific application, positioning it as a reliable tool in clinical practice.

In the field of guided surgery, although the studies showed promising accuracy (over 94%) and precision (over 87%), the protocols employed were relatively simple. For this technology to gain widespread clinical adoption, it will be essential to refine and validate more complex functionalities.

AI applications in prognosis showed more variable results, indicating the need for further research and development to improve reliability in some areas. However, in other aspects, the technology appears more optimized and ready for clinical use as a support to the clinician.

Ethical approval

Not required.

Patient consent

Not required.

Funding

This work was supported by the BIK-AINTEK program of the Basque Government under Grant no. 007-B2/2021.

Competing interests

None.

Declaration of Competing Interest

No conflicts of interest declared.

Appendix A. Supporting information

Supplementary data associated with this article can be found in the online version at [doi:10.1016/j.ijom.2025.04.005](https://doi.org/10.1016/j.ijom.2025.04.005).

References

- Agrawal P, Nikhade P. Artificial intelligence in dentistry: past, present, and future. *Cureus* 2022;14:e27405. <https://doi.org/10.7759/cureus.27405>
- Sun ML, Liu Y, Liu G, Cui D, Heidari AA, Jia WY, Ji X, Chen H, Luo Y. Application of machine learning to stomatology: a comprehensive review. *IEEE Access* 2020;8:184360–74. <https://doi.org/10.1109/ACCESS.2020.3028600>
- Yang WF, Su YX. Artificial intelligence-enabled automatic segmentation of skull CT facilitates computer-assisted craniomaxillofacial surgery. *Oral Oncol* 2021;118:105360. <https://doi.org/10.1016/j.oraloncology.2021.105360>
- Sarker IH. Deep learning: a comprehensive overview on techniques, taxonomy, applications and research directions. *SN Comput Sci* 2021;2:420. <https://doi.org/10.1007/s42979-021-00815-1>
- Lecun Y, Bengio Y, Hinton G. Deep learning. *Nature* 2015;521:436–44. <https://doi.org/10.1038/nature14539>
- Alqutaibi AY, Algabri RS, Elawady D, Ibrahim WI. Advancements in artificial intelligence algorithms for dental implant identification: a systematic review with meta-analysis. *J Prosthet Dent* 2023. <https://doi.org/10.1016/j.prosdent.2023.11.027>. [Epub ahead of print].
- Mohammad-Rahimi H, Motamedian SR, Pirayesh Z, Haiat A, Zahedrozegar S, Mahmoudinia E, Rohban MH, Krois J, Lee JH, Schwendicke F. Deep learning in periodontology and oral implantology: a scoping review. *J Periodontol Res* 2022;57:942–51. <https://doi.org/10.1111/jre.13037>
- Chaurasia A, Namachivayam A, Koca-Ünsal RB, Lee JH. Deep-learning performance in identifying and classifying dental implant systems from dental imaging: a systematic review and meta-analysis. *J Periodontol Implant Sci* 2024;54:3–12. <https://doi.org/10.5051/jpis.2300160008>
- Dashti M, Londono J, Ghasemi S, Tabatabaei S, Hashemi S, Baghaei K, Palma PJ, Khurshid Z. Evaluation of accuracy of deep learning and conventional neural network algorithms in detection of dental implant type using intraoral radiographic images: a systematic review and meta-analysis. *J Prosthet Dent* 2025;133:137–46. <https://doi.org/10.1016/j.prosdent.2023.11.030>
- Ibraheem WI. Accuracy of artificial intelligence models in dental implant fixture identification and classification from radiographs: a systematic review. *Diagnostics* 2024;14:806. <https://doi.org/10.3390/diagnostics14080806>
- Alqutaibi AY, Algabri R, Ibrahim WI, Alhajj MN, Elawady D. Dental implant planning using artificial intelligence: a systematic review and meta-analysis. *J Prosthet Dent* 2024. <https://doi.org/10.1016/j.prosdent.2024.03.032>. [Epub ahead of print].
- Moons KGM, Wolff RF, Riley RD, Whiting PF, Westwood M, Collins GS, Reitsma JB, Kleijnen J, Mallett S. PROBAST: a tool to assess risk of bias and applicability of prediction model studies: explanation and elaboration. *Ann Intern Med* 2019;170:W1–33. <https://doi.org/10.7326/M18-1377>
- Moher D, Liberati A, Tetzlaff J, Altman DG, PRISMA Group. Preferred reporting items for systematic reviews and meta-analyses: the PRISMA statement. *PLoS Med* 2009;6:e1000097. <https://doi.org/10.1371/journal.pmed.1000097>
- Couso-Queiruga E, Mansouri CJ, Alade AA, Allareddy TV, Galindo-Moreno P, Avila-Ortiz G. Alveolar ridge preservation reduces the need for ancillary bone augmentation in the context of implant therapy. *J Periodontol* 2022;93:847–56. <https://doi.org/10.1002/JPER.22-0030>
- Sakai T, Li H, Shimada T, Kita S, Iida M, Lee C, Nakano T, Yamaguchi S, Imazato S. Development of artificial intelligence model for supporting implant drilling protocol decision making. *J Prosthodont Res* 2023;67:360–5. https://doi.org/10.2186/jpr.JPR_D_22_00053
- Türker H, Aksoy B, Özsoy K. Fabrication of customized dental guide by stereolithography method and evaluation of dimensional accuracy with artificial neural networks. *J Mech Behav Biomed Mater* 2022;126:105071. <https://doi.org/10.1016/j.jmbbm.2021.105071>
- Hashem M, Mohammed ML, Youssef AE. Improving the efficiency of dental implantation process using guided local search models and continuous time neural networks with robotic assistance. *IEEE Access* 2020;8:202755–64. <https://doi.org/10.1109/ACCESS.2020.3034689>
- Yang X, Xie J, Li X, Li X, Shen L, Deng Y. TCSLoT: text guided 3D context and slope aware triple network for dental implant position prediction. arXiv: 2308.05355. arXiv; 2023.
- Yang X, Li X, Li X, Wu P, Shen L, Deng Y. ImplantFormer: vision transformer-based implant position regression using dental CBCT data. *Neural Comput Appl* 2024;36:6643–58. <https://doi.org/10.1007/s00521-023-09411-1>
- Başaran M, Çelik Ö, Bayrakdar IS, Bilgir E, Orhan K, Odabaş A, Aslan AF, Jagtap R. Diagnostic charting of panoramic radiography using deep-learning artificial intelligence system. *Oral Radiol* 2022;38:363–9. <https://doi.org/10.1007/s11282-021-00572-0>
- Jang WS, Kim S, Yun PS, Jang HS, Seong YW, Yang HS, Chang JS. Accurate detection for dental implant and peri-implant tissue by transfer learning of faster R-CNN: a diagnostic accuracy study. *BMC Oral Health* 2022;22:591. <https://doi.org/10.1186/s12903-022-02539-x>
- De Angelis F, Pranno N, Franchina A, Di Carlo S, Brauner E, Ferri A, Pellegrino G, Grecchi E, Goker F, Stefanelli LV. Artificial intelligence: a new diagnostic software in dentistry: a preliminary performance diagnostic study. *Int J Environ Res Public Health* 2022;19:1728. <https://doi.org/10.3390/ijerph19031728>
- Chen SL, Chen TY, Mao YC, Lin SY, Huang YY, Chen CA, Lin YJ, Hsu YM, Li CA, Chiang WY, Wong KY, Abu PAR. Automated detection system based on convolution neural networks for retained root, endodontic treated teeth, and implant recognition on dental panoramic images. *IEEE Sens J* 2022;22:23293–232306. <https://doi.org/10.1109/JSEN.2022.3211981>
- Al-Ghamdi ASAM, Ragab M, AlGhamdi SA, Asseri AH, Mansour RF, Koundal D. Detection of dental diseases through X-ray images using neural search architecture network. *Comput Intell Neurosci* 2022;2022:3500552. <https://doi.org/10.1155/2022/3500552>
- Bonfanti-Gris M, Garcia-Cañas A, Alonso-Calvo R, Salido Rodriguez-Manzaneque MP, Pradies Ramiro G. Evaluation of an artificial intelligence web-based software to detect and classify dental structures and treatments in panoramic radiographs. *J Dent* 2022;126:104301. <https://doi.org/10.1016/j.jdent.2022.104301>
- Vera M, Gómez-Silva MJ, Vera V, López-González CI, Aliaga I, Gascó E,

- Vera-González V, Pedrera-Canal M, Besada-Portas E, Pajares G. Artificial intelligence techniques for automatic detection of peri-implant marginal bone remodeling in intraoral radiographs. *J Digit Imaging* 2023;**36**:2259–77. <https://doi.org/10.1007/s10278-023-00880-3>
27. Gardiyanoglu E, Ünsal G, Akkaya N, Aksoy S, Orhan K. Automatic segmentation of teeth, crown–bridge restorations, dental implants, restorative fillings, dental caries, residual roots, and root canal fillings on orthopantomographs: convenience and pitfalls. *Diagnostics* 2023;**13**:1487. <https://doi.org/10.3390/diagnostics13081487>
 28. Elgarba BM, Van Aelst S, Swaita A, Morgan N, Shujaat S, Jacobs R. Deep learning-based segmentation of dental implants on cone-beam computed tomography images: a validation study. *J Dent* 2023;**137**:104639. <https://doi.org/10.1016/j.jdent.2023.104639>
 29. Chen YC, Chen MY, Chen TY, Chan ML, Huang YY, Liu YL, Lee PT, Lin GJ, Li TF, Chen CA, Chen SL, Li KC, Abu PAR. Improving dental implant outcomes: CNN-based system accurately measures degree of peri-implantitis damage on periapical film. *Bioengineering* 2023;**10**:640. <https://doi.org/10.3390/bioengineering10060640>
 30. Orhan K, Aktuna Belgin C, Manulis D, Golitsyna M, Bayrak S, Aksoy S, Sanders A, Önder M, Ezhov M, Shamshiev M, Gusarev M, Shlenskii V. Determining the reliability of diagnosis and treatment using artificial intelligence software with panoramic radiographs. *Imaging Sci Dent* 2023;**53**:199–208. <https://doi.org/10.5624/isd.20230109>
 31. Singh NK, Faisal M, Hasan S, Goswami G, Raza K. A single-stage deep learning approach for multiple treatment and diagnosis in panoramic X-ray. In: Abraham A, Bajaj A, Hanne T, Siarry P, editors. *Lecture notes in networks and systems*, 1046 LNNS. Springer; 2024. p. 233–42.
 32. Lee DW, Kim SY, Jeong SN, Lee JH. Artificial intelligence in fractured dental implant detection and classification: evaluation using dataset from two dental hospitals. *Diagnostics* 2021;**11**:233. <https://doi.org/10.3390/diagnostics11020233>
 33. Cha JY, Yoon HI, Yeo IS, Huh KH, Han JS. Panoptic segmentation on panoramic radiographs: deep learning-based segmentation of various structures including maxillary sinus and mandibular canal. *J Clin Med* 2021;**10**:2577. <https://doi.org/10.3390/jcm10122577>
 34. Choi H, Jeon KJ, Kim YH, Ha EG, Lee C, Han SS. Deep learning-based fully automatic segmentation of the maxillary sinus on cone-beam computed tomographic images. *Sci Rep* 2022;**12**:14009. <https://doi.org/10.1038/s41598-022-18436-w>
 35. Zeng P, Song R, Lin Y, Li H, Chen S, Shi M, Cai G, Gong Z, Huang K, Chen Z. Abnormal maxillary sinus diagnosing on CBCT images via object detection and “straight-forward” classification deep learning strategy. *J Oral Rehabil* 2023;**50**:1465–80. <https://doi.org/10.1111/joor.13585>
 36. Liu Y, Xie R, Wang L, Liu H, Liu C, Zhao Y, Bai S, Liu W. Fully automatic AI segmentation of oral surgery-related tissues based on cone beam computed tomography images. *Int J Oral Sci* 2024;**16**:34. <https://doi.org/10.1038/s41368-024-00294-z>
 37. ak H, Kim D, Gil SY. Automatic sagittal plane detection for the identification of the mandibular canal. *J Korea Comput Graph Soc* 2020;**26**:31–7. <https://doi.org/10.15701/kcgs.2020.26.3.31>
 38. Jaskari J, Sahlsten J, Järnstedt J, Mehtonen H, Karhu K, Sundqvist O, Hietanen A, Varjonen V, Mattila V, Kaski K. Deep learning method for mandibular canal segmentation in dental cone beam computed tomography volumes. *Sci Rep* 2020;**10**:5842. <https://doi.org/10.1038/s41598-020-62321-3>
 39. Maheswari PU, Banumathi A, Priya K. Detection of inferior alveolar nerve canal by feature based machine learning approach. *J Phys Conf Ser* 2021;**1917**:012025. <https://doi.org/10.1088/1742-6596/1917/1/012025>
 40. Järnstedt J, Sahlsten J, Jaskari J, Kaski K, Mehtonen H, Lin Z, Hietanen A, Sundqvist O, Varjonen V, Mattila V, Prapayasotok S, Nalampang S. Comparison of deep learning segmentation and multigrader-annotated mandibular canals of multicenter CBCT scans. *Sci Rep* 2022;**12**:18598. <https://doi.org/10.1038/s41598-022-20605-w>
 41. Widiarsi M, Arifin AZ, Suciati N, Faticah C, Astuti ER, Indraswari R, Putra RH, Za'in C. Dental-YOLO: alveolar bone and mandibular canal detection on cone beam computed tomography images for dental implant planning. *IEEE Access* 2022;**10**:101483–94. <https://doi.org/10.1109/ACCESS.2022.3208350>
 42. Usman M, Rehman A, Saleem AM, Jawaid R, Byon SS, Kim SH, Lee BD, Heo MS, Shin YG. Dual-stage deeply supervised attention-based convolutional neural networks for mandibular canal segmentation in CBCT scans. *Sensors* 2022;**22**:9877. <https://doi.org/10.3390/s22249877>
 43. Maheswari PU, Banumathi A, Ulaganathan G, Yoganandha R. Inferior alveolar nerve canal segmentation by local features based neural network model. *IET Image Process* 2022;**16**:703–16. <https://doi.org/10.1049/ipr2.12375>
 44. Tian G, Song X. Y. Mandibular canal segmentation from CBCT image using 3D convolutional neural network with scSE attention. *IEEE Access* 2022;**10**:111272–83. <https://doi.org/10.1109/ACCESS.2022.3213839>
 45. Jindanil T, Marinho-Vieira LE, de-Azevedo-Vaz SL, Jacobs R. A unique artificial intelligence-based tool for automated CBCT segmentation of mandibular incisive canal. *Dentomaxillofac Radiol* 2023;**52**:20230321. <https://doi.org/10.1259/dmfr.20230321>
 46. Widiarsi M, Suciati N, Faticah C, Astuti ER, Putra RH, Arifin AZ. *Alveolar bone and mandibular canal segmentation on cone beam computed tomography images using U-Net*. Proceedings of the 2023 international conference on instrumentation, control, and automation, ICA 2023. Institute of Electrical and Electronics Engineers; 2023. p. 36–41.
 47. Oliveira-Santos N, Jacobs R, Picoli FF, Lahoud P, Niclaes L, Groppo FC. Automated segmentation of the mandibular canal and its anterior loop by deep learning. *Sci Rep* 2023;**13**:10819. <https://doi.org/10.1038/s41598-023-37798-3>
 48. Yang S, Li A, Li P, Yun Z, Lin G, Cheng J, Xu S, Qiu B. Automatic segmentation of inferior alveolar canal with ambiguity classification in panoramic images using deep learning. *Heliyon* 2023;**9**:e13694. <https://doi.org/10.1016/j.heliyon.2023.e13694>
 49. Ntovas P, Marchand L, Finkelman M, Revilla-León M, Att W. Accuracy of artificial intelligence-based segmentation of the mandibular canal in CBCT. *Clin Oral Implants Res* 2024;**35**:1163–71. <https://doi.org/10.1111/clr.14307>
 50. Fang X, Zhang S, Wei Z, Wang K, Yang G, Li C, Han M, Du M. Automatic detection of the third molar and mandibular canal on panoramic radiographs based on deep learning. *J Stomatol Oral Maxillofac Surg* 2024;**125**(4S):101946. <https://doi.org/10.1016/j.jormas.2024.101946>
 51. Raza H, Ali M, Singh VK, Wahjuningrum A, Sarig R, Chaurasia A. Segmentation of mental foramen in orthopantomographs: a deep learning approach. arXiv:2408.04763. arXiv; 2024.
 52. Ni FD, Xu ZN, Liu MQ, Zhang MJ, Li S, Bai HL, Ding P, Fu KY. Towards clinically applicable automated mandibular canal segmentation on CBCT. *J Dent* 2024;**144**:104931. <https://doi.org/10.1016/j.jdent.2024.104931>
 53. Sorkhabi MM, Saadat Khajeh M. Classification of alveolar bone density

- using 3-D deep convolutional neural network in the cone-beam CT images: a 6-month clinical study. *Measurement* 2019;**148**:106945. <https://doi.org/10.1016/j.measurement.2019.106945>
54. Widiarsi M, Arifin AZ, Suciati N, Astuti ER, Indraswari R. *Alveolar bone detection from dental cone beam computed tomography using YOLOv3-tiny*. AIMS 2021—international conference on artificial intelligence and mechatronics systems. Institute of Electrical and Electronics Engineers; 2021.
 55. Xiao Y, Liang Q, Zhou L, He X, Lv L, Chen J, Endian S, Jianbin G, Wu D, Lin L. Construction of a new automatic grading system for jaw bone mineral density level based on deep learning using cone beam computed tomography. *Sci Rep* 2022;**12**:12841. <https://doi.org/10.1038/s41598-022-16074-w>
 56. Park CS, Kang SR, Kim JE, Huh KH, Lee SS, Heo MS, Han JJ, Yi WJ. Validation of bone mineral density measurement using quantitative CBCT image based on deep learning. *Sci Rep* 2023;**13**:11921. <https://doi.org/10.1038/s41598-023-38943-8>
 57. Lee JH, Yun JH, Kim YT. Deep learning to assess bone quality from panoramic radiographs: the feasibility of clinical application through comparison with an implant surgeon and cone-beam computed tomography. *J Periodontal Implant Sci* 2024;**54**:349–58. <https://doi.org/10.5051/JPLIS.2302880144>
 58. Abu Marar RF, Uliyan DM, Al-Sewadi HA. Mandible bone osteoporosis detection using cone-beam computed tomography. *Eng Technol Appl Sci Res* 2020;**10**:6027–33.
 59. Gong Z, Li X, Shi M, Cai G, Chen S, Ye Z, Gan X, Yang R, Wang R, Chen Z. Measuring the binary thickness of buccal bone of anterior maxilla in low-resolution cone-beam computed tomography via a bilinear convolutional neural network. *Quant Imaging Med Surg* 2023;**13**:8053–66. <https://doi.org/10.21037/qims-23-744>
 60. Gurses A, Oktay AB. Tooth restoration and dental work detection on panoramic dental images via CNN. In: Proceedings of the 2020 medical technologies congress (TIPTEKNO); 2020. p. 1–4.
 61. Çelik B, Çelik ME. Automated detection of dental restorations using deep learning on panoramic radiographs. *Dentomaxillofac Radiol* 2022;**51**:20220244. <https://doi.org/10.1259/dmfr.20220244>
 62. Adnan N, Hanif M, Khan K, Faridoon F, Umer F. An artificial intelligence model for implant segmentation on periapical radiographs. *J Pak Med Assoc* 2024;**74**(4 (Supple-4)):S5–9. <https://doi.org/10.47391/JPMA.AKU-9S-02>
 63. Maged S, Adel A, Tawfik M, Badawy W. Dental diagnostics—a YOLOv8-based framework. In: 2024 international conference on machine intelligence and smart innovation, ICMISI 2024—proceedings. institute of electrical and electronics engineers; 2024. p. 144–7.
 64. Li W, Wang Y, Liu Y. DMAF-Net: deformable multi-scale adaptive fusion network for dental structure detection with panoramic radiographs. *Dentomaxillofac Radiol* 2024;**53**:296–307. <https://doi.org/10.1093/dmfr/twae014>
 65. Bonfanti-Gris M, Herrera A, Paraiso-Medina S, Alonso-Calvo R, Martínez-Rus F, Pradies G. Performance evaluation of three versions of a convolutional neural network for object detection and segmentation using a multiclass and reduced panoramic radiograph dataset. *J Dent* 2024;**144**:104891. <https://doi.org/10.1016/j.jdent.2024.104891>
 66. Mantravadi A, Raj K, Pawar R, R. SCT, S. NK. Spatial field fusion network (SFFNet) for panoramic dental X-ray segmentation. In: Proceedings of the 2023 IEEE applied sensing conference (APSCON); 2023. p. 1–3.
 67. Kohinata K, Kitano T, Nishiyama W, Mori M, Iida Y, Fujita H, Katsumata A. Deep learning for preliminary profiling of panoramic images. *Oral Radiol* 2023;**39**:275–81. <https://doi.org/10.1007/s11282-022-00634-x>
 68. Nie Q, Li C, Yang J, Yao Y, Sun H, Jiang T, Grzegorzec M, Chen A, Chen H, Hu W, Li R, Zhang J, Wang D. OIIDS: a benchmark oral implant image dataset for object detection and classification evaluation. *Comput Biol Med* 2023;**167**:107620. <https://doi.org/10.1016/j.compbiomed.2023.107620>
 69. Lee JH, Kim YT, Lee JB, Jeong SN. A performance comparison between automated deep learning and dental professionals in classification of dental implant systems from dental imaging: a multi-center study. *Diagnostics* 2020;**10**:910. <https://doi.org/10.3390/diagnostics10110910>
 70. Sukegawa S, Yoshii K, Hara T, Yamashita K, Nakano K, Yamamoto N, Nagatsuka H, Furuki Y. Deep neural networks for dental implant system classification. *Biomolecules* 2020;**10**:984. <https://doi.org/10.3390/biom10070984>
 71. Hadj Saïd M, Le Roux MK, Catherine JH, Lan R. Development of an artificial intelligence model to identify a dental implant from a radiograph. *Int J Oral Maxillofac Implants* 2020;**36**:1077–82. <https://doi.org/10.11607/jomi.8060>
 72. Lee JH, Jeong SN. Efficacy of deep convolutional neural network algorithm for the identification and classification of dental implant systems, using panoramic and periapical radiographs: a pilot study. *Medicine* 2020;**99**:e20787. <https://doi.org/10.1097/MD.00000000000020787>
 73. Takahashi T, Nozaki K, Gonda T, Mamenno T, Wada M, Ikebe K. Identification of dental implants using deep learning—pilot study. *Int J Implant Dent* 2020;**6**:53. <https://doi.org/10.1186/s40729-020-00250-6>
 74. Kim JE, Nam NE, Shim JS, Jung YH, Cho BH, Hwang JJ. Transfer learning via deep neural networks for implant fixture system classification using periapical radiographs. *J Clin Med* 2020;**9**:1117. <https://doi.org/10.3390/jcm9041117>
 75. da Mata Santos RP, Vieira Oliveira Prado HE, Soares Aranha Neto I, Alves de Oliveira GA, Vespasiano Silva AI, Zenóbio EG, Manzi FR. Automated identification of dental implants using artificial intelligence. *Int J Oral Maxillofac Implants* 2021;**36**:918–23. <https://doi.org/10.11607/jomi.8684>
 76. Lee JH, Kim YT, Lee JB, Jeong SN. Deep learning improves implant classification by dental professionals: a multi-center evaluation of accuracy and efficiency. *J Periodontal Implant Sci* 2022;**52**:220–9. <https://doi.org/10.5051/jpis.2104080204>
 77. Benakatti VB, Nayakar RP, Anandhalli M. Machine learning for identification of dental implant systems based on shape—a descriptive study. *J Indian Prosthodont Soc* 2021;**21**:405–11. https://doi.org/10.4103/jips.jips_324_21
 78. Sukegawa S, Yoshii K, Hara T, Matsuyama T, Yamashita K, Nakano K, Takabatake K, Kawai H, Nagatsuka H, Furuki Y. Multi-task deep learning model for classification of dental implant brand and treatment stage using dental panoramic radiograph images. *Biomolecules* 2021;**11**:815. <https://doi.org/10.3390/biom11060815>
 79. Kong HJ, Yoo JY, Eom SH, Lee JH. Deep learning algorithms for identifying 79 dental implant types. *J Dent Rehab Appl Sci* 2022;**38**:196–203.
 80. Kohlakala A, Coetzer J, Bertels J, Vandermeulen D. Deep learning-based dental implant recognition using synthetic X-ray images. *Med Biol Eng Comput* 2022;**60**:2951–68. <https://doi.org/10.1007/s11517-022-02642-9>
 81. Ayman A, Arafat SW, Eldin AMH, Atia A. Dental implant recognition and classification with convolutional neural network. In: Proceedings of the 2022 2nd international mobile, intelligent, and ubiquitous computing conference (MIUCC); 2022. p. 477–82.
 82. Sukegawa S, Yoshii K, Hara T, Tanaka F, Yamashita K, Kagaya T, Nakano K, Takabatake K, Kawai H, Nagatsuka H, Furuki Y. Is attention branch network effective in classifying dental implants

- from panoramic radiograph images by deep learning? *PLoS One* 2022; **17**:e0269016. <https://doi.org/10.1371/journal.pone.0269016>
83. Kim HS, Ha EG, Kim YH, Jeon KJ, Lee C, Han SS. Transfer learning in a deep convolutional neural network for implant fixture classification: a pilot study. *Imaging Sci Dent* 2022;**52**:219–24. <https://doi.org/10.5624/isd.20210287>
 84. Park W, Huh JK, Lee JH. Automated deep learning for classification of dental implant radiographs using a large multi-center dataset. *Sci Rep* 2023;**13**:4862. <https://doi.org/10.1038/s41598-023-32118-1>
 85. Kong HJ. Classification of dental implant systems using cloud-based deep learning algorithm: an experimental study. *J of Yeungnam Med Sci* 2023; **40**(Suppl.):S29–36. <https://doi.org/10.12701/jyms.2023.00465>
 86. Park JH, Moon HS, Jung HI, Hwang J, Choi YH, Kim JE. Deep learning and clustering approaches for dental implant size classification based on periapical radiographs. *Sci Rep* 2023;**13**:16856. <https://doi.org/10.1038/s41598-023-42385-7>
 87. Tiryaki B, Ozdogan A, Guller MT, Miloglu O, Oral EA, Ozbek IY. Dental implant brand and angle identification using deep neural networks. *J Prosthet Dent* 2023. <https://doi.org/10.1016/j.prosdent.2023.07.022>. [Epub ahead of print].
 88. Kong HJ, Eom SH, Yoo JY, Lee JH. Identification of 130 dental implant types using ensemble deep learning. *Int J Oral Maxillofac Implants* 2023;**38**:150–6. <https://doi.org/10.11607/jomi.9818>
 89. Park W, Schwendicke F, Krois J, Huh JK, Lee JH. Identification of dental implant systems using a large-scale multi-center data set. *J Dent Res* 2023; **102**:727–33. <https://doi.org/10.1177/00220345231160750>
 90. Kong HJ, Yoo JY, Lee JH, Eom SH, Kim JH. Performance evaluation of deep learning models for the classification and identification of dental implants. *J Prosthet Dent* 2023. <https://doi.org/10.1016/j.prosdent.2023.07.009>. [Epub ahead of print].
 91. Huang X, Chen X, Zhong X, Tian T. The CNN model aided the study of the clinical value hidden in the implant images. *J Appl Clin Med Phys* 2023; **24**:e14141. <https://doi.org/10.1002/acm2.14141>
 92. Lubbad MAH, Kurtulus IL, Karaboga D, Kilic K, Basturk A, Akay B, Nalbantoglu OU, Yilmaz OMD, Ayata M, Yilmaz S, Pacal I. A comparative analysis of deep learning-based approaches for classifying dental implants decision support system. *J Imaging Inform Med* 2024;**37**:2559–80. <https://doi.org/10.1007/s10278-024-01086-x>
 93. Leblebicioglu Kurtulus I, Lubbad M, Yilmaz OMD, Kilic K, Karaboga D, Basturk A, Akay B, Nalbantoglu U, Yilmaz S, Ayata M, Pacal I. A robust deep learning model for the classification of dental implant brands. *J Stomatol Oral Maxillofac Surg* 2024; **125**(S51):101818. <https://doi.org/10.1016/j.jormas.2024.101818>
 94. Hassan NA, Kamel AE, Omran AE, Gad MW, Ashraf NM, Ahmed OM, Abdel-Fattah MA. Automated identification of dental implants: a new, fast and accurate artificial intelligence system. *Eur J Prosthodont Restor Dent* 2024;**32**:162–7. https://doi.org/10.1922/EJPRD_2620Hassan06
 95. Lee JH, Kim YT, Lee JB. Identification of dental implant systems from low-quality and distorted dental radiographs using AI trained on a large multi-center dataset. *Sci Rep* 2024;**14**:12606. <https://doi.org/10.1038/s41598-024-63422-z>
 96. Arijji Y, Kusano K, Fukuda M, Wakata Y, Nozawa M, Kotaki S, Arijji E, Baba S. Two-step deep learning models for detection and identification of the manufacturers and types of dental implants on panoramic radiographs. *Odontology* 2024. <https://doi.org/10.1007/s10266-024-00989-z>. [Online ahead of print].
 97. Ou-Yang S, Han S, Sun D, Wu H, Chen J, Cai Y, Yin D, Ou-Yang H, Liao L. The preliminary in vitro study and application of deep learning algorithm in cone beam computed tomography image implant recognition. *Sci Rep* 2023; **13**:18467. <https://doi.org/10.1038/s41598-023-45757-1>
 98. Kurt Bayrakdar S, Orhan K, Bayrakdar IS, Bilgir E, Ezhov M, Gusarev M, Shumilov E. A deep learning approach for dental implant planning in cone-beam computed tomography images. *BMC Med Imaging* 2021;**21**:86. <https://doi.org/10.1186/s12880-021-00618-z>
 99. Lin Y, Shi M, Xiang D, Zeng P, Gong Z, Liu H, Liu Q, Chen Z, Xia J, Chen Z. Construction of an end-to-end regression neural network for the determination of a quantitative index sagittal root inclination. *J Periodontol* 2022;**93**:1951–60. <https://doi.org/10.1002/JPER.21-0492>
 100. Roongruangsilp P, Khongkhunthian P. The learning curve of artificial intelligence for dental implant treatment planning: a descriptive study. *Appl Sci* 2021;**11**:10159. <https://doi.org/10.3390/app112110159>
 101. Park J, Lee J, Moon S, Lee K. Deep learning based detection of missing tooth regions for dental implant planning in panoramic radiographic images. *Appl Sci* 2022;**12**:1595. <https://doi.org/10.3390/app12031595>
 102. Bodhe R, Sivakumar S, Raghuvanshi A. Design and development of deep learning approach for dental implant planning. 2022 international conference on green energy, computing and sustainable technology, GECOST 2022. Institute of Electrical and Electronics Engineers; 2022. p. 269–74.
 103. Alsomali M, Alghamdi S, Alotaibi S, Alfadda S, Altwaijry N, Alturaiki I, Al-Ekrish A. Development of a deep learning model for automatic localization of radiographic markers of proposed dental implant site locations. *Saudi Dent J* 2022;**34**:220–5. <https://doi.org/10.1016/j.sdentj.2022.01.002>
 104. Chang HC, Yu LW, Liu BY, Chang PC. Classification of the implant–ridge relationship utilizing the MobileNet architecture. *J Dent Sci* 2024;**19**:411–8. <https://doi.org/10.1016/j.jds.2023.08.002>
 105. Moufti MA, Trabulsi N, Ghousheh M, Fattal T, Ashira A, Danishvar S. Developing an artificial intelligence solution to autosegment the edentulous mandibular bone for implant planning. *Eur J Dent* 2023;**17**:1330–7. <https://doi.org/10.1055/s-0043-1764425>
 106. Hwang IK, Kang SR, Yang S, Kim JM, Kim JE, Huh KH, Lee SS, Heo MS, Yi WJ, Kim TI. SinusC-Net for automatic classification of surgical plans for maxillary sinus augmentation using a 3D distance-guided network. *Sci Rep* 2023; **13**:11653. <https://doi.org/10.1038/s41598-023-38273-9>
 107. Yang X, Xie J, Li X, Li X, Li X, Shen L, Deng Y. TCEIP: text condition embedded regression network for dental implant position prediction. arXiv: 2306.14406. arXiv; 2023.
 108. Yang X, Li X, Li X, Chen W, Shen L, Li X, Deng Y. Two-stream regression network for dental implant position prediction. *Expert Syst Appl* 2024;**235**:121135. <https://doi.org/10.1016/j.eswa.2023.121135>
 109. Lee S, Woo S, Yu J, Seo J, Lee J, Lee C. Automated CNN-based tooth segmentation in cone-beam CT for dental implant planning. *IEEE Access* 2020; **8**:50507–18. <https://doi.org/10.1109/ACCESS.2020.2975826>
 110. Al-Asali M, Alqutaibi AY, Al-Sarem M, Saeed F. Deep learning-based approach for 3D bone segmentation and prediction of missing tooth region for dental implant planning. *Sci Rep* 2024; **14**:13888. <https://doi.org/10.1038/s41598-024-64609-0>
 111. Elgarba BM, Fontenele RC, Ali S, Swaity A, Meeus J, Shujaat S, Jacobs R. Validation of a novel AI-based automated multimodal image registration of CBCT and intraoral scan aiding pre-surgical implant planning. *Clin Oral Implants Res* 2024;**35**:1506–17. <https://doi.org/10.1111/clr.14338>

112. Yang X, Li X, Luo X, Zeng L, Zhang Y, Shen L, Deng Y. Simplify implant depth prediction as video grounding: a texture perceive implant depth prediction network. arXiv:2406.04603. MICCAI'2024. arXiv; 2024. (<https://doi.org/10.48550/arXiv.2406.04603>).
113. Ha SR, Park HS, Kim EH, Kim HK, Yang JY, Heo J, Yeo IL. A pilot study using machine learning methods about factors influencing prognosis of dental implants. *J Adv Prosthodont* 2018; **10**:395–400. <https://doi.org/10.4047/jap.2018.10.6.395>
114. Liu CH, Lin CJ, Hu YH, You ZH. Predicting the failure of dental implants using supervised learning techniques. *Appl Sci* 2018; **8**:698. <https://doi.org/10.3390/app8050698>
115. Lyakhov PA, Dolgalev AA, Lyakhova UA, Muraev AA, Zolotayev KE, Semerikov DY. Neural network system for analyzing statistical factors of patients for predicting the survival of dental implants. *Front Neuroinform* 2022; **16**:1067040. <https://doi.org/10.3389/fninf.2022.1067040>
116. Huang N, Liu P, Yan Y, Xu L, Huang Y, Fu G, Lan Y, Yang S, Song J, Li Y. Predicting the risk of dental implant loss using deep learning. *J Clin Periodontol* 2022; **49**:872–83. <https://doi.org/10.1111/jcpe.13689>
117. Zhang C, Fan L, Zhang S, Zhao J, Gu Y. Deep learning based dental implant failure prediction from periapical and panoramic films. *Quant Imaging Med Surg* 2023; **13**:935–45. <https://doi.org/10.21037/qims-22-457>
118. Oh S, Kim YJ, Kim J, Jung JH, Lim HJ, Kim BC, Kim KG. Deep learning-based prediction of osseointegration for dental implant using plain radiography. *BMC Oral Health* 2023; **23**:208. <https://doi.org/10.1186/s12903-023-02921-3>
119. Xie C, Li Y, Liu K, Liu J, Zeng J, Huang N, Yang S. A hybrid unsupervised clustering method for predicting the risk of dental implant loss. *J Dent* 2024; **149**:105260. <https://doi.org/10.1016/j.jdent.2024.105260>
120. Rajan RSS, Kumar HSK, Sekhar A, Nadakkavukaran D, Feroz SMA, Gangadharappa P. Evaluating the role of AI in predicting the success of dental implants based on preoperative CBCT images: a randomized controlled trial. *J Pharm Bioallied Sci* 2024; **16**(1):S886–8. https://doi.org/10.4103/jpbs.jpbs_1117_23
121. Lin CH, Wang HL, Yu LW, Chou PY, Chang HC, Chang CH, Chang PC. Deep learning for the identification of ridge deficiency around dental implants. *Clin Implant Dent Relat Res* 2024; **26**:376–84. <https://doi.org/10.1111/cid.13301>
122. Zhang H, Shan J, Zhang P, Chen X, Jiang H. Trabeculae microstructure parameters serve as effective predictors for marginal bone loss of dental implant in the mandible. *Sci Rep* 2020; **10**:18437. <https://doi.org/10.1038/s41598-020-75563-y>
123. Cha JY, Yoon HI, Yeo IS, Huh KH, Han JS. Peri-implant bone loss measurement using a region-based convolutional neural network on dental periapical radiographs. *J Clin Med* 2021; **10**:1–12. <https://doi.org/10.3390/jcm10051009>
124. Liu M, Wang S, Chen H, Liu Y. A pilot study of a deep learning approach to detect marginal bone loss around implants. *BMC Oral Health* 2022; **22**:11. <https://doi.org/10.1186/s12903-021-02035-8>
125. Troiano G, Fanelli F, Rapani A, Zotti M, Lombardi T, Zhurakivska K, Stacchi C. Can radiomic features extracted from intra-oral radiographs predict physiological bone remodelling around dental implants? A hypothesis-generating study. *J Clin Periodontol* 2023; **50**:932–41. <https://doi.org/10.1111/jcpe.13797>
126. Riberti N, Furlani M, D'Amico E, Comuzzi L, Piattelli A, Iezzi G, Giuliani A. Deep learning for microstructural characterization of synchrotron radiation-based collagen bundle imaging in peri-implant soft tissues. *Appl Sci* 2023; **13**:4423. <https://doi.org/10.3390/app13074423>
127. Wang CW, Hao Y, Di Gianfilippo R, Sugai J, Li J, Gong W, Kornman KS, Wang HL, Kamada N, Xie Y, Giannobile WV, Lei YL. Machine learning-assisted immune profiling stratifies peri-implantitis patients with unique microbial colonization and clinical outcomes. *Theranostics* 2021; **11**:6703–16. <https://doi.org/10.7150/thno.57775>
128. Mameno T, Wada M, Nozaki K, Takahashi T, Tsujioka Y, Akema S, Hasegawa D, Ikebe K. Predictive modeling for peri-implantitis by using machine learning techniques. *Sci Rep* 2021; **11**:11090. <https://doi.org/10.1038/s41598-021-90642-4>
129. Lee WF, Day MY, Fang CY, Nataraj V, Wen SC, Chang WJ, Teng NC. Establishing a novel deep learning model for detecting peri-implantitis. *J Dent Sci* 2024; **19**:1165–73. <https://doi.org/10.1016/j.jds.2023.11.017>
130. Alharbi MT, Almutiq MM. Prediction of dental implants using machine learning algorithms. *J Health Eng* 2022; **2022**:7307675. <https://doi.org/10.1155/2022/7307675>
131. Huang Z, Zheng H, Huang J, Yang Y, Wu Y, Ge L, Wang L. The construction and evaluation of a multi-task convolutional neural network for a cone-beam computed-tomography-based assessment of implant stability. *Diagnostics* 2022; **12**:2673. <https://doi.org/10.3390/diagnostics12112673>
132. Yadalam PK, Trivedi SS, Krishnamurthi I, Anegundi RV, Mathew A, Shayeb MA, Narayanan JK, Jaber MA, Rajkumar R. Machine learning predicts patient tangible outcomes after dental implant surgery. *IEEE Access* 2022; **10**:131481–8. <https://doi.org/10.1109/ACCESS.2022.3228793>
133. Kwack DW, Park SM. Prediction of medication-related osteonecrosis of the jaw (MRONJ) using automated machine learning in patients with osteoporosis associated with dental extraction and implantation: a retrospective study. *J Korean Assoc Oral Maxillofac Surg* 2023; **49**:135–41. <https://doi.org/10.5125/jkaoms.2023.49.3.135>
134. He K, Zhang X, Ren S, Sun J. Deep residual learning for image recognition. In: Proceedings of the IEEE computer society conference on computer vision and pattern recognition. Vol. 2016-December. IEEE Computer Society; 2016. p. 770–8.
135. Girshick R, Donahue J, Darrell T, Malik J. Rich feature hierarchies for accurate object detection and semantic segmentation. In: Proceedings of the 2014 IEEE conference on computer vision and pattern recognition (CVPR); 2014.
136. Szegedy C, Liu W, Jia Y, Sermanet P, Reed S, Anguelov D, Erhan D, Vanhoucke V, Rabinovich A. Going deeper with convolutions. In: Proceedings of the IEEE computer society conference on computer vision and pattern recognition. IEEE Computer Society; 2015.
137. Simonyan K, Zisserman A. Very deep convolutional networks for large-scale image recognition. In: Third international conference on learning representations, ICLR 2015 – conference track proceedings. International Conference on Learning Representations (ICLR); 2014.
138. Redmon J, Divvala S, Girshick R, Farhadi A. You only look once: unified, real-time object detection. In: Proceedings of the 2016 IEEE conference on computer vision and pattern recognition (CVPR); 2016.
139. Ronneberger O, Fischer P, Brox T. U-Net: convolutional networks for biomedical image segmentation. Lecture notes in computer science (including subseries lecture notes in artificial intelligence and lecture notes in bioinformatics). 9351. Springer; 2015. p. 234–41.
140. Freund Y, Schapire RE. A decision-theoretic generalization of on-line learning and an application to boosting. Lecture notes in computer science (including

- subseries lecture notes in artificial intelligence and lecture notes in bioinformatics). 904. Springer; 1995. p. 23–37.
141. Cortes C, Vapnik V. Support-vector networks. *Mach Learn* 1995;**20**:273–97.
 142. Cox D. The regression analysis of binary sequences. *J R Stat Society: Ser B (Methodol)* 1958;**20**:215–32. <https://doi.org/10.1111/j.2517-6161.1958.tb00292.x>
 143. Breiman L. Random forests. *Mach Learn* 2001;**45**:5–32.
 144. Lewis DD. *Naive (Bayes) at forty: the independence assumption in information retrieval. Lecture notes in computer science (including subseries lecture notes in artificial intelligence and lecture notes in bioinformatics)* 1398. Springer; 1998. p. 4–15.
 145. Fix E, Hodges J. Discriminatory analysis—nonparametric discrimination: consistency properties. *Int Stat Inst (ISI)* 1989;**57**:238–47. <https://doi.org/10.2307/1403797>
 146. Howard AG, Zhu M, Chen B, Kalenichenko D, Wang W, Weyand T, Andreetto M, Adam H. MobileNets: efficient convolutional neural networks for mobile vision applications. arXiv:1704.04861. arXiv; 2017.
 147. Tan M, Le QV. EfficientNet: rethinking model scaling for convolutional neural networks. arXiv:1905.11946. arXiv; 2019.
 148. Krizhevsky A, Sutskever I, Hinton GE. ImageNet classification with deep convolutional neural networks. In: Pereira F, Burges CJ, Bottou L, Weinberger KQ, editors. *Advances in neural information processing systems*, 25. Curran Associates; 2012.
 149. Huang G, Liu Z, Van Der Maaten L, Weinberger KQ. Densely connected convolutional networks. In: Proceedings of the 30th IEEE conference on computer vision and pattern recognition, CVPR 2017. Vol. 2017-January. Institute of Electrical and Electronics Engineers; 2017. p. 2261–9.
 150. Chollet F. Xception: deep learning with depthwise separable convolutions. In: Proceedings of the 2017 IEEE conference on computer vision and pattern recognition (CVPR); 2017.

Correspondence to: Department of Computer Science and Artificial Intelligence
 University of the Basque Country (UPV/EHU)
 Paseo de Manuel Lardizabal
 1
 Donostia-San Sebastian
 20018
 Spain.
 Tel.: +34 686974038.
 E-mail: gvazquez004@ikasle.ehu.eus